List of key requirements and recommendations for the design of the well completion

D 8.3

List of key requirements and recommendations for the design of the well completion

D 8.3

Version 1.0

Part I – Michal Kruszewski, Volker Wittig

Part II – Michal Kruszewski, Giordano Montegrossi, Francesco Parisio, Erik H. Saenger

Part III – Michal Kruszewski, Giordano Montegrossi, Marvin Glissner, Volker Wittig

Work package 8

27 April 2020

Website: http://www.gemex-h2020.eu

The GEMex project is supported by the European Union's Horizon 2020 programme for Research and Innovation under grant agreement No 727550

Table of Contents[1]

[1] The content of this report reflects only the authors' view. The Innovation and Networks Executive Agency (INEA) is not responsible for any use that may be made of the information it contains.

List of figures

List of tables

Executive summary

Work package 8 aims to develop and verify concepts and technologies to access and exploit super-hot reservoirs (i.e., geothermal resources with temperature conditions >380 °C, including conditions above the critical point). In particular, this WP aims to summarize the existing knowledge and derive steps necessary for the development of such an unconventional resource. Drilling into a super-hot geothermal system requires specific measures, including e.g., pressure control or appropriate wellbore sealant material. Similarly, well completion will not only need to take into account material properties of casing strings and casing connections but also the thermal stresses caused by drilling and reheating of the well during production. An analysis of the requirements for the drilling under the conditions of the presumed super-hot resource in the Los Humeros reservoir was performed in this report including drilling monitoring and borehole measurements. The know-how collected in this study shall enable the geothermal community to be able to tap into hot reservoirs by avoiding common mistakes and have possible solutions at hand for challenges and problems within such super-hot regimes.

This report is composed of three main parts. The first part presents a comprehensive review of super-hot drilling campaigns carried out worldwide with their failure modes, recommendations, and already implemented improvements in regard to drilling and well completion technology. The review includes know-how derived from project partners and super-hot locations such as Iceland (IDDP-1 and -2, IMAGE, DEEPEGS), Italy (DESCRAMBLE), or Japan (Japan Beyond Brittle). The second part describes an investigation on the local in-situ stress tensor of the Los Humeros geothermal field based on borehole observations. The final aim of this part is to contribute to a better understanding of yet poorly understood local in-situ stress field of the Los Humeros volcanic complex. This investigation is considered useful for the assessment and management of the seismic risks, exploration, and exploitation of deep geothermal energy, including super-hot resources of the Los Humeros geothermal field. Third and the last part, describes the development of a model for prediction of the cement sheath failure in super-hot wells, based on an example of the H-64 well, drilled in the central parts of the Los Humeros caldera. In the last part of this report, the results of the experimental laboratory studies performed on wellbore sealants based on alkali-activated alumiono-silicates were presented. Such non-Portland sealants are proposed as potential alternatives to the conventional Ordinary Portland Cement blend types for the well completions of the future super-hot geothermal wells.

Acknowledgments

Authors would like to thank CFE in Morelia, especially to Marcela Sánchez Luviano and Miguel Ramírez Montes, for cooperation, constructive conversations, and data from the Los Humeros geothermal field, without which this report would not be possible. Authors would like to thank Thomas Reinsch from the GFZ German Research Centre for Geosciences, Gunnar Skúlason Kaldal from the Iceland GeoSurvey, Sverrir Þórhallsson from the Keilir Institute of Technology for their knowledge, support, and constructive criticism and conversations during the preparation of this report. Authors would like to thank Dimitrios Mendrinos from the Centre for Renewable Energy Sources and Saving for sharing his experience regarding Greek geothermal expeditions in Milos and Nisyros and Egill Juliusson from Landsvirkjun for sharing his experience from the KJ-39 well in northern Iceland. Authors would like to express deep gratitude to the late Ruggero Bertani from the ENEL Green Power for sharing his experience from the Venelle-2 deep drilling campaign. Additional thanks go to Matteo Loizzo for his valuable and constructive suggestions and comments, especially from the area of wellbore integrity and cement quality analysis, given during the preparation of this report. Authors would like to also thank Maurice Lefebvre for helping with the laboratory work and Hochschule Bochum for providing the laboratory equipment and support.

1 Review of Failure Models in Supercritical Geothermal Drilling Projects

(Michal Kruszewski, Volker Wittig)

This work has been published in: Kruszewski M., Wittig V., Review of failure modes in supercritical geothermal drilling projects, Geothermal Energy, Science – Society – Technology, 6:28, 2018, DOI 10.1186/s40517-018-0113-4.

1.1 Introduction

Conventional hydrothermal wells with a depth of around 3000 m and temperatures of 340 °C can yield from 4 up to 10 MW_e. Recent studies have proven that productivity might be increased by a factor of 10 if fluids from supercritical resources had been extracted (Friðleifsson et al., 2005, 2014a, b). This is due to the increased enthalpy, lower viscosity, and density of supercritical fluids that allow for much higher flow rates. The longevity of a geothermal well drilled into the supercritical resource depends significantly on the appropriate drilling and well completion technology. Deep and high- temperature drilling projects in countries such as Iceland, Italy, Kenya, Japan, Greece, USA, and Mexico have all reached critical temperatures and encountered, in the majority, highly corrosive and hostile fluids. Such extreme reservoir conditions promoted damage to the casing material, cement sheaths, surface equipment, and led to serious well failures and in many cases to well abandonment. These drilling campaigns created an acute need for improvements in drilling and well completion technologies being currently used for high-temperature wells.

It is worth emphasizing, at this point, the great ambiguity of terms ‘supercritical’, ‘superheated’ and ‘super-hot’ geothermal resources. Up to this date, there is no clear definition available of what is considered as ‘supercritical’ or ‘super-hot’ geothermal resource. In the Oxford English Dictionary, word ‘supercritical’ is described as ‘relating to or denoting a fluid at a temperature and pressure greater than its critical temperature and pressure’, whereas the Academic Press Dictionary of Science and Technology explains the word ‘supercritical’ as ‘the mobile phase of a substance intermediate between liquid and vapor, maintained at a temperature greater than its critical point’. It can be seen, that depending on the source, ‘supercritical’ fluids might be regarded as exceeding critical temperature only or simultaneously exceeding critical pressure and temperature. This proves the great ambiguity of a ‘supercritical’ geothermal resource and its confusion within the scientific world.

To assume drilling into supercritical resources, one must always consider the chemical composition of the reservoir fluids present. The critical temperature and pressure increase significantly with salinity, transferring the supercritical conditions to much greater depths. The critical point of pure water is achieved at 374 °C and 221 bars and assuming boiling conditions starting from the well surface, corresponds to a drilling depth of 3500 m, as presented in Figure 1. The critical point of seawater, i.e., 3.5 % NaCl as indicated by Bischoff and Rosenbauer (1984) is reached at 405 °C and 302 bars and corresponds to a depth of approximately 5300 m assuming boiling conditions starting from the well surface. In the case of a geothermal reservoir

with low or non-existent vertical permeability, pressure conditions may be governed by the hydrostatic pressure of a cold water column only, or by the lithostatic pressure so that the critical pressure of the fluid will be reached at a depths between 2300 and 3000 m assuming seawater salinity (Elders et al., 2014). This phenomenon is confirmed by the existence of black smokers (i.e., hydrothermal vents) in the rift zones at the bottom of oceans expelling fluids at temperatures exceeding 400 °C without boiling conditions occurring (Bischoff et al., 1984).

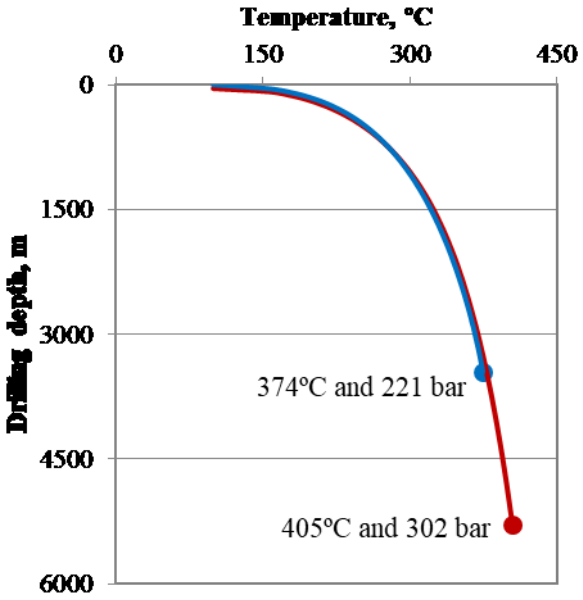

Figure 1: Critical temperature and pressure points for pure water (blue line) and saltwater (red line).

Other researchers underline the significant influence of reservoir permeability and its great value to the amount of energy and volume of fluid that can be extracted from the geothermal resource. According to Scott et al. (2015), supercritical resources are those areas of a geothermal system, where reservoir permeability is higher than 10^{-16} m^2 as well as the specific enthalpy and the temperature of the water is greater than its critical point. Such definition avoids including pressure as a criterion for a supercritical resource and applies no distinction between 'superheated' (i.e., pressure conditions below critical point) and 'supercritical' (i.e., pressure conditions above critical point) resources. This explanation seems to be the most accurate, as currently there are no commercial geothermal fields that produce pure water only; thus, the pressure of 221 bars is not a very relevant criterion. Out of 20 drilling ventures mentioned in this research, only a few simultaneously reached and confirmed the pressure and temperature of the geothermal fluid present higher than its critical point, i.e., the recent IDDP-2 well in Reykjanes (Iceland) and the Venelle-2 drilling venture in southern Tuscany (Italy). For instance, the well IID-14 in the Salton Sea geothermal field (USA) reached a temperature of 390 °C, which is several hundred degrees Celsius lower than that of any supercritical brine that could be present in that field with a total amount of dissolved fluids of approximately 25, 000 mg/kg (Elders & Sass, 1998; Ross 1991).

Even greater ambiguity concerns the 'super-hot' geothermal resources. This term has been used within the GEMex, where 'super-hot geothermal systems' are regarded as geothermal wells

experiencing ambient temperatures higher than 380 °C, and the planned Newberry Deep Drilling Project (NDDP) where 'super-hot' resources were regarded as geothermal wells with temperatures higher than 400 °C (Cladouhos et al., 2018). Similarly, to 'supercritical' resources, 'super-hot' resources do not have a clear definition within the scientific community and remain ambiguous.

To make some generalization to the drilling projects being revised in this study and due to the lack of solid information regarding reservoir permeability, measured downhole pressure conditions and chemical composition of the reservoir fluid present of the particular geothermal fields being investigated, authors will consider the criterion of critical temperature of the pure water only for determining a supercritical geothermal resource.

A failure mode is regarded as any kind of damage to the downhole construction (e.g., casing strings, a cement sheath) and/or surface equipment (e.g., wellhead) of a geothermal well that either temporarily excludes further drilling operations, well testing or fluid production, or leads directly to the partial or total well abandonment. All of the geothermal wells drilled into extremely high temperatures push their components including casing strings, casing connections, wellhead assembly, cement sheaths, drilling fluid to its technical limits. Based on the classification of casing failures made by Teodoriu (2015), excluding casing failure from corrosion, extensive wear, and overloading, most wells investigating high-temperature geothermal resources will fall into the category of the so-called temperature variation induced fatigue. This kind of failure is caused by large temperature variations and is aggravated by the lack of casing mobility within the cement sheaths. It is expected, that such casing failure will be caused by accumulated temperature cycles, putting the casing material above its yield limit. Similarly, to the casing material and connections, fatigue due to extensive thermally driven loads will lead to cement sheaths damage and loss of the cement bond at casing-cement or cement-rock interfaces with the potential influx of hostile reservoir fluids.

Geothermal wells may be categorized based on the ambient well temperatures (Böðvarsson 1961) into low temperature with less than 150 °C at 1000 m, medium temperature between 150 °C and 200 °C at 1000 m and high temperature with conditions equal or higher than 200 °C at 1000 m. There has been, however, an increasing number of boreholes, drilled in the conditions greatly exceeding this categorization, with multiple wells reaching resources with temperatures close to or exceeding the critical temperatures of pure water. Figure 2 represents the relation between reservoir pressure and temperature of selected geothermal wells from different high-enthalpy locations worldwide, which are close to or exceeded supercritical conditions of pure (blue line) or sea (red line) water. It can be seen that only a few wells have exceeded simultaneously critical temperatures and pressures. It is worth mentioning that different temperature measuring techniques were applied depending on the reservoir conditions and, at the time, available logging equipment and methods. For instance, the temperature in the IDDP-2 well in the Reykajnes geothermal field (Iceland) was measured using the wire-line technology near the well bottom; whereas in the IDDP-1 well in the Krafla geothermal field (Iceland), the temperature was measured during well discharge operations at the well surface, and in the WD-

1A well in the Kakkonda geothermal field (Japan) temperature was measured, amongst other methods, using melting points of pure tellurium metal lowered into the well.

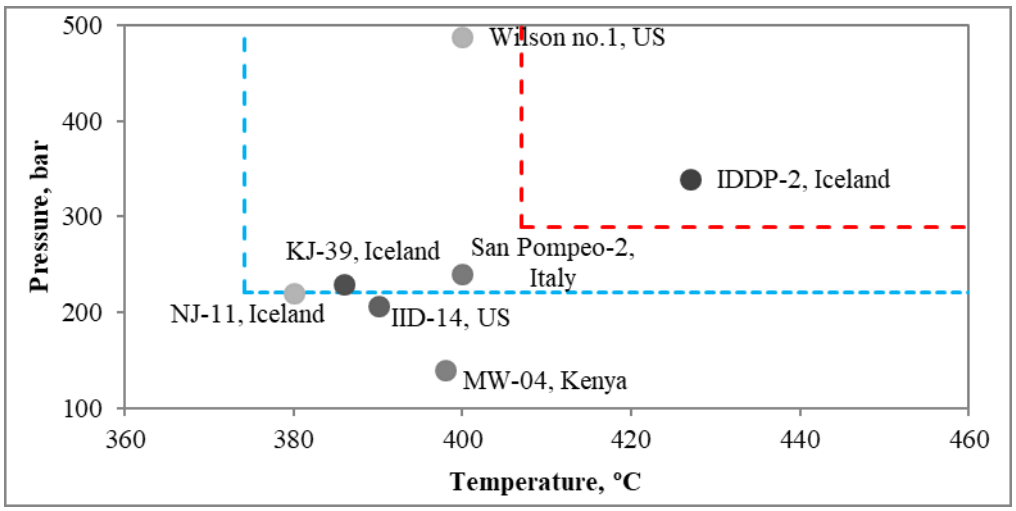

Figure 2: Maximum reservoir temperatures and pressures measured in geothermal wells, where supercritical conditions were encountered (blue line – the critical point of clean water, red line – the critical point of seawater).

The casing program is the most crucial feature that influences successful drilling operations and the longevity of the future geothermal fluid production. It implies assessing casing setting depths, a number of casing strings, nominal casing weight, casing material, type of connections and well completion. The main functions of casing programs are preventing casing deformation, supporting blow-out preventers and permanent wellhead, containing drilling and production fluids, preventing groundwater contamination, mitigating drilling fluid losses, protecting wells from corrosion, fracturing, and erosion, preventing inter-zonal cross-contamination of geothermal fluids, defining a production zone and providing access to the reservoir (New Zealand Standard 2015). Conventional high-temperature geothermal wells consist usually of three to four cemented casing strings. The typical casing program for most geothermal wells incorporates a conductor pipe, a surface casing, an intermediate casing which may serve as an anchor casing (i.e., casing string to which wellhead is attached), a production casing and an optional perforated liner (holed or slotted). All of these casing strings mentioned are cemented from casing shoe to top of casing string in order to prevent corrosion resulting from the migration of reservoir fluids and to control thermal expansion during fluid production. A liner pipe, which is either suspended from a liner hanger or set at the well bottom, is usually left uncemented in the production section of the well. The completion is finalized by assembling a permanent wellhead at the top of the well. In most cases, it includes an expansion spool placed directly below the first master valve, which allows for expansion of the uppermost parts of the production casing string with respect to the anchor casing to which the permanent wellhead is attached.

No reliable and well-established methods and criteria for well design are yet available for wells with temperatures close to or exceeding the critical point for pure water. The New Zealand Code of Practice for Deep Geothermal Wells from 2015 covers geothermal well design with

an account of material strength reduction for well temperatures only up to 350 °C (Karlsson 1978) and production of non-corrosive geothermal fluids. Such temperatures, as previously demonstrated, have already been exceeded in multiple super-hot locations around the world and in many cases, the produced fluids were highly corrosive and acidic.

Up to this date, no research has focused exclusively on drilling and well completion aspects of geothermal wells exploring supercritical resources. This study is a follow-up and extension of the work carried out by Reinsch et al. (2017) focusing on current research efforts and potential opportunities that supercritical geothermal resources might provide for international collaboration as well as presenting a list of past supercritical drilling ventures. Authors strongly believe that a thorough investigation of previous case scenarios and their challenges, as carried out in this paper, will be crucial to harness thermal energy from the supercritical geothermal reservoirs in the future in the safest possible manner.

The paper is divided into three distinguishable sections. The first section presents an overview of the recently undertaken international initiatives for exploring supercritical geothermal resources together with their main goals. The second section gives a detailed review of well histories together with the description of failures being encountered. The third section presents authors' recommendations and already implemented improvements of the current drilling and completion technologies being applied for drilling high-temperature wells worldwide in order to safely and more efficiently harness supercritical geothermal resources.

1.2 International cooperation for exploring supercritical geothermal resources

Supercritical geothermal resources are currently being investigated in many areas worldwide within joint international programs, driven mostly by the European initiatives. A brief description of few such programs is presented below.

DESCRAMBLE[2] was an international drilling project aiming to investigate supercritical resources within the Larderello geothermal field in southern Tuscany (Italy). The main goal of the project was to drill into a supercritical geothermal resource, test and demonstrate new drilling techniques, control gas emissions, high temperatures and pressures expected from the deep geothermal reservoir as well as to characterize their chemical and thermo-physical conditions. The recently finished Venelle-2 well achieved temperatures of more than 500 °C at a well depth of 2810 m measured using various techniques.

The aim of the DEEPEGS[3] project was to demonstrate the feasibility of EGS for delivering energy from renewable resources within Europe. Drilling of the IDDP-2 well in south-west Iceland was the first step to investigate such unconventional resources. The IDDP-2 well was able to go beyond critical pressure and temperature of saline geothermal waters of the Reykjanes reservoir and achieved a temperature of 427 °C at depth of approximately 4600 m and perform the deepest primary reverse cementation in Iceland and one of the deepest in the

[2] http://www.descramble-h2020.eu/
[3] http://deepegs.eu/

world at approximately 3000 m of depth. The IDDP-2 well is currently the deepest and hottest well in Iceland.

The main objective of the Japan Beyond Brittle Project (JBBP) was to demonstrate enhanced geothermal energy extraction through the scientific understanding of various phenomena in the brittle-ductile transition. This research was preceded by the initial deep drilling of the WD-1A geothermal well conducted at the Kakkonda geothermal field between 1994 and 1995, which have proven very low permeability. Drilling operations were eventually withheld due to safety reasons and possible gas ejection (Asanuma et al., 2015).

1.3 Review of past case studies

This section describes histories of high-enthalpy geothermal wells in different super-hot locations worldwide with reservoir temperatures exceeding the critical point of pure water, which have experienced one or more failures modes. Detailed technical specification of presented wells (i.e., date of drilling, final depth, temperature and pressure conditions, logging methods and failure modes) are presented in Table 1, together with their casing programs and parameters such as casing setting depths, casing materials, nominal weights and types of casing connections used.

Greece

The Nisyros-1 wildcat well was drilled in 1982 on the Greek island of Nisyros to the final depth of 1816 m. A temperature of approximately 400 °C was measured directly on the wellhead assembly. Production from Nisyros-1 was carried out from two zones, with a deeper one containing brines of very high salinity of approximately 100 g/kg of total dissolved solids. The casing design process was performed assuming formation temperatures being equal to boiling curves of 10 to 25 % NaCl brines. After performing the first production tests, the 9 5/8" production casing was seriously damaged at six different intervals between a depth of approximately 150 and 1240 m and plugged with scale deposits. It is worth to mention that no treatment other than circulating drilling fluid was done, before placing and cementing to mitigate circulation losses. Due to the buckled sections of the casing, collapsed areas were re-drilled with a milling assembly and a remedial 7" tie-back casing was placed to a depth of 1258 m. During the next production tests, the newly installed 7" tie-back casing also experienced casing collapse and buckling (Chiotis and Vrellis, 1995). These two cases of casing failure can be explained by fast heating during initial production tests and fast cooling during well killing operations with cold water exerting extremely high thermal loads upon cemented casing strings. The casing failures are also likely to be associated with bad primary cementing operations which might have been caused by rock fracturing and corrosion resulted from highly saline reservoir fluids (personal communication with Dimitrios Mendrinos). It was concluded from the chemical composition of the productive horizons that high overpressures exist at shallow and greater depths, resulting in a high probability of a blow-out. The Nisyros-2 well, drilled in the close vicinity to the Nisyros-1 well, did not experienced casing collapse, which can be explained by the experience gained in this area and changes to the well design including

implementation of steel with a higher yield strength (Geothermica Italiana 1983; 1984; Mendrinos et al., 2010).

Iceland

The NJ-11 well in the Nesjavellir geothermal field was drilled in 1985 to a final depth of 2265 m. During drilling operations, multiple overpressurized feed zones were encountered which later resulted in circulation gain and wellhead pressure rise of 5 – 6 bars after circulation ceased. First fluid losses and main feed zone were found at a depth of 1226 m. Immediately after drilling, geothermal fluids with a flow rate of 35 l/s, flowed up the annulus between casing and drill string. This rather unexpected incident had to be quenched with cold water. After a temperature survey, accompanied by pumping 44 l/s of cold water into the well, interzonal flow and possible underground blow-out conditions occurred. It was observed that potentially supercritical fluids, with pressures above 220 bars and temperatures of more than 380 °C were entering the main feed zone at 1226 m. High temperatures damaged the float valve in the drill string and fluid leakage was observed on top of the lubricator at the wellhead assembly. Controlling the well after drilling operations with cold water proved to be immensely difficult and unsuccessful. The NJ-11 well was partially abandoned by inserting a 200 m plug made from gravel and the well was eventually completed with a slotted liner down to the top of the gravel plug. The well was later produced from upper aquifers (Steingrimsson et al., 1986). The experience gained from the NJ-11 well led to the creation of the Iceland Deep Drilling Project (IDDP) to further investigate supercritical geothermal fluids. The location of the NJ-11 well is currently being considered as a prospect for the third IDDP deep drilling campaign.

The KJ-39 well was drilled directionally to a final depth of 2865 m in the Krafla geothermal field in northern Iceland in 2008. Recovery of cuttings amounted to 100 % from drilling to 1400 m and became partial between depths of 1400 and 2650 m. In deeper well sections, total circulation losses were experienced. After reaching the target depth, the drill string got stuck for a week and had to be freed with the use of explosives. Once the drill string was retrieved from the well, the lower units of the bottom hole assembly contained up to 30 % of freshly quenched glass, indicating drilling into magma. The ambient well temperature of approximately 386 °C was measured using a wire-line logging tool at a depth of 2822 m, indicating supercritical temperatures. Eventually, the lower part of the K-39 well was sealed off with a cement plug, due to the possible threats of the lower zone being highly acidic, causing potential well damage (Árnadóttir et al., 2009; Mortensen et al., 2010). After retrieving parts of the liner pipe from the well, heavy corrosion was observed (Figure 3). The construction of the KJ-39 well proved to be incapable of withstanding the conditions anticipated from a deeper and much more powerful aquifer (Einarsson et al., 2010). Pressure measurements from deeper well sections are unavailable. As of August 2013, the KJ-39 well was turned into an injection well within the Krafla geothermal field (personal communication with Egill Juliusson).

Figure 3: Heavy corrosion of liner pipe in the KJ-39 well (source: deliverable D4.3 from GeoWell project, Thorbjornsson 2016).

The main aim of the first experiment of the IDDP in the Krafla geothermal field in northern Iceland was to drill to a target depth of 4500 m, in order to produce from supercritical geothermal resource. The IDDP-1 well was designed specifically to be capable of handling the extreme temperature and pressure conditions, which wells NJ-11 and KJ-39 were not able to withstand (Þórhallsson et al., 2003, 2010). Drilling of the IDDP-1 well was performed without major problems up to 2000 m and proved to be extremely challenging after reaching that depth with multiple loss circulation zones, a failed coring attempt, stuck pipe incidents due to drilling into rhyolite magma that required multiple side-tracking and created obstacles during the primary cementing operation. The cementing job of an anchor casing failed mainly due to the total circulation losses. After a cement bond log (CBL) tool was run, 200 m of a void in the cement sheath was discovered, between depths of 1410 and 1600 m. An inflatable packer, used primarily to cement sacrificial production casing, failed to keep sufficient pressures and reverse balance cementing job had to be performed. The IDDP-1 well was eventually completed at 2072 m with a final well depth of 2104 m. The maximum temperatures measured at the wellhead assembly amounted to 450 °C with a pressure of 142 bars, making the IDDP-1, the hottest geothermal well in Iceland and one of the hottest in the world (Pálsson et al., 2014). After a period of extensive flow testing, the well had to be quenched with cold water due to the malfunction of two master valves at the well surface, and further testing was terminated. Even with rather slow and careful killing, thermal stresses, exerted upon sacrificial casing were significantly high and the casing experienced collapse at two sections below 600 m, with possible other at deeper well sections, and casing couplings rupture. Other problems experienced were corrosion of casing material, extensive scaling (especially visible in the

surface equipment as presented in Figure 4), erosion and eccentric casing. The IDDP-1 well was eventually abandoned (Friðleifsson et al., 2014a, b; Ingason et al., 2014). There is a proposal to further investigate the magma encountered in the IDDP-1 well by the Krafla Magma Testbed[4] (KMT) project which aims at characterizing the physical, chemical, and mechanical properties of the interval between the hydrothermal system and magma and possibly develop methods of heat extraction directly from a magma source.

Figure 4: Heavy silica scaling in the surface equipment of the IDDP-1 well during discharge testing (Karlsdottir et al., 2015).

Drilling operation for the second IDDP well started in August 2016 with a deepening of an existing 2500 m deep production RN-15 well located in the Reykjanes geothermal field in south-west Iceland. The RN-15 was a mere vertical production well with a 13 3/8" production casing string cemented down to 794 m with an open hole completion. Drilling of the IDDP-2 well was carried out 'blind' i.e., without any drilling fluid returns with an exception of an interval of around 180 m after completed primary cementing operation of an anchor casing at 2941 m depth. Losses of drilling fluid could not be cured with loss circulation material (i.e., polymer pills) nor with multiple cement plugs performed through drill bit and through drillable fiber cementing strings. Multiple challenges occurred during drilling operations including weather delays, problems with hole instability that required multiple reaming jobs as well as stuck pipe incidents. The IDDP-2 well was cemented using reverse circulation method, due to total fluid losses and achieved satisfactory results. As of today, the IDDP-2 well has the deepest cemented casing in any geothermal well in Iceland. 13 core runs were attempted with rather poor core recovery using an impregnated 8 ½" diamond core bit and perfect core recovery of nearly 100 % with a 6" PDC core bit beneath the liner pipe. Poor core recovery in the IDDP-2 well might be explained by fill-in at the bottom of the well, inclination, heavy dog legs, thermal fracturing of the rock formations as well as the diameter of core barrel being wider than the diameter of heavyweight drill pipe. The IDDP-2 well was finished at a depth of 4659 m in mid-December 2016 and the perforated liner pipe was lowered to a well depth of 4572 m. At the end of drilling operations, an additional sacrificial 7" casing was set to a depth of 1300 m and cemented. Logging program, including temperature, pressure, and injectivity measurements,

[4] https://www.kmt.is/

was carried out after 6 days of partial heating up. It was confirmed that the IDDP-2 well successfully penetrated the supercritical conditions of the geothermal brines in the Reykjanes geothermal system with 427 °C and 340 bars of pressure. The main feed zones of the IDDP-2 well were estimated at depths of 3360 m, 4200 m, 4370 m and 4550 m (Friðleifsson & Elders, 2017; Friðleifsson et al., 2017). Right after the drilling operation ceased, a 3 ½" injection string was lowered close to the well bottom and a 5-months stimulation operation with cold water pumping started. In May 2017, temperature logs were carried out after a few days of heating up and confirmed bottom hole temperature of approximately 535 °C. After well stimulation, an attempt was made to seal off the main feed zone at 3400 m using biodegradable polymers. Unexpectedly, material blocked the well from downflowing, and cooling was no longer possible. This resulted in week-long heating up of the production casing string and serious casing damage at depth between 2307 and 2380 m was discovered with wire-line logs. After retrieving the stimulation string, corrosion of latter assembly sections was observed.

Italy

The San Pompeo 2 exploration well was drilled in 1979 to identify the deep production zones down to the 3000 m reflector. The operations were carried out with a total loss of circulation starting from a depth of 836 m to the bottom of the well. Any attempt of plugging the rock formation fractures to stop circulation loss during drilling proved to be unsuccessful. Several drill string failures occurred while drilling, mainly due to corrosion from hydrogen expelled from the reservoir. During drilling at a depth of 2930 m, a violent hydrogen gas explosion was experienced. After the blow-out, well collapsed and only the first 2560 m of the well depth was accessible for further testing due to rock debris left at the well bottom. The well experienced another similar blow-out incident right after drilling operations restarted. Samples from deep geothermal fluids proved the presence of hostile gases and a strongly corrosive environment (Barbier 1984). Temperature and pressure conditions proved the presence of a superheated geothermal resource, i.e., 394 °C and 212 bars at 2560 m of depth. The materials, as well as drilling and production procedures available at the time of drilling, were considered not suitable for such harsh downhole conditions and the San Pompeo 2 well was eventually abandoned.

Table 1: Casing programs of geothermal wells where temperature above critical point of pure water has been encountered.

Country	Well	Year	Depth, m	Temp., °C	Press., bar	Depth of the measurement, m	Measurement method	Failure mode	Casing program					Reference
									Surface	Intermediate	Anchor	Production	Liner pipe	
Italy	*Sasso-22*	1980	4094	380	n/n	3970	Wire-line logs	High well temperatures	24”	-	18 5/8” @400m	13 3/8” @1400m	9 5/8” @2900m	(Bertini et al., 1980)
	San Pompeo-2	1979	2996	395	>240	2560	n/n	Blow-out	n/n	n/n	n/n	n/n	n/n	(Barbier 1984)
	San Vito-1	1980	3045	419	n/n	2500	Zinc sheet	Wellhead not rated for supercritical conditions	20”, J55, BTC @147m	13 3/8” , J55, BTC @1009m	9 5/8”, C75, Hydril @2025m	Liner 7”, J55, BTC @1897-2487m (liner)	6”, J55 @2382-3045m (slotted liner)	(Baron et al., 1980)
	Venelle-2	2017	2900	>500	n/n	2810	Wire-line Kuster KTG tool (and 444° C with SINTEF PT tool, 480-610 °C at 2894m with thermosensitive paints)	Blow-out; cementing equipment failure	18 5/8”, J55, Tenaris ER, 133 lb/ft @182m	-	13 3/8“, L80 (13 %Cr), Tenaris ER, 68 lb.ft @1029m	Liner 9 5/8“, L80, TSH ER, 44 lb/ft @1000-2300m	Liner 7“, T95, TSH Blue, 29 lb/ft @2250-2800m	(Bertani et al., 2018)
											9 5/8“, L80, TSH ER, 44 lb/ft @1000m (tie-back)	Liner 7“, TN125SS, TSH Blue, 32 lb/ft @1100-2250m	Open hole @3000-3500m	
												Tie-back 7”, TN125SS, 32 lb/ft, TSH Blue @1100m		

	Carboli-11	1990	3455	427	n/n	3328	Melting alloy	n/n	n/n	n/n	n/n	n/n	n/n	(Ruggieri et al., 1995)
Iceland	*NJ-11*	1985	2265	>380	>220	1900 (tool deflection)	Wire-line with 44 l/s of cold water pumped into annulus	Underground blow-out	18 5/8" @54m	-	13 3/8", 61, 68 lb/ft, K55 @183m	9 5/8", 43lb/ft, K55, BTC @566m	7" 24 lb/ft, K55, BTC @561-1617m	(Steingrimsson et al., 1986)
	IDDP-1	2008	2104	450	142	At wellhead during well discharge		Wellhead valve failure, casing rupture due to well quenching, corrosion and precipitation	32 ½", X56, welded, @87m	24 ½" 162lb/ft, K55, welded, @254m 18 5/8", 114lb/ft, K55, BTC @785m	13 5/8", 88lb/ft, T95, Hydril 563 @290m 13 3/8", 72lb/ft, K55, Hydril 563 @290-1949m	9 5/8", 54lb/ft, K55, Hydril @563-1935m (sacrificial)	9 5/8", 47lb/ft, K55, BTC @1935-2072m (part of production casing)	(Þórhallsson et al., 2014)
	IDDP-2	2016	4659	427	340	4560	Wire-line logs; 6 days after drilling with 40 l/s fluid pumping	Casing damage	22 ½", 117lb/ft, X56, welded @87m	18 5/8", X56, welded @293m 13 3/8", 68lb/ft, K55, BTC @794m	9 7/8", 63lb/ft, T95, GEOCONN @535m 9 5/8", 47 lb/ft, L80, GEOCONN @535-2941m	7", 26lb/ft, TN 80HS, Hydril @1303m (sacrificial)	7", 26lb/ft, L80, BTC @2941-4572m	(Ingason et al., 2015) (Friðleifsson et al., 2017a; 2017b)
	KJ-39	2008	2858	386	230	2822	Wire-line shortly after	Well construction not rated for	18 5/8" @74m	-	13 5/8", K55, BTC @282m	9 5/8" @967m	7", K55, BTC @2608m	(Mortensen et al., 2010)

							drilling within stuck drill string	supercritical condition; in operation as an injection well						
Japan	*WD-1A*	1994	3729	500	n/n	>3500	Melting points of pure tellurium metal	Safety concerns due to H_2S and CO_2 ejection	18 5/8", @600m	-	13 3/8", @1500m	9 5/8" @1363-2546m	Open hole	(Saito et al., 1998)
USA	*Wilson No 1*	1981	3672	400	489	2980, 3350	Fluid inclusions	Casing collapse	20", 94lb/ft, H40, seamless, Vetco @50m	-	13 3/8" K-55. 68 and 55lb/ft, -K55, BTC, @894m	9 5/8", 40, 44, 47, 54 lb/ft L80 and K-55 @2804m	Open hole	(DOGGR reports 1982) (Fournier 1991)
	Prati-32	2010	3396	400	n/n	3352	From steam entry	In operation as injection well	22" @98m	16 1/8" @912m	11 3/4" @1863m	8 5/8" (liner) @2591-3048m	7" @3048-3388m with 5" (blank liner) @2590m	(Garcia 2015)
	IID-14	1990	2073	390	207	2073	Wire-line logs	n/n	16" @114m	-	-	9 5/8" @302m	7" @789m	(DOGGR reports 1990)
	KS-13	2005	2488	1050	n/n	2844	Dacite magma temperature	In operation as injection well	20" 94lb/ft, K55, BTC @305m	-	13 3/8", 61 lb/ft, K55, VAM @610	9 5/8", 47lb/ft, C-90, VAM @1189m	7", 29lb/ft, L80, BTC @1159m	(Teplow 2009)
Mexico	*H-43*	2007	2200	395	113	2200	Wire-line during	Precipitation and erosion	20" K-55 94lb/ft, BTC @47m	-	13 3/8" K-55 54.5lb/ft, BTC @501m	9 5/8" L-80 47 lb/ft, BTC @1245m	Open hole	(Diez et al., 2015)

							heating-up							
Kenya	*MW-01*	2011	2206	391	n/n	n/n	n/n	n/n	20" @81m	-	13 3/8" @400m	9 5/8" @840m	7" @2206m (slotted liner)	(Okwiri 2013), (Khaemba 2015) (Mbia 2014) (Kipyego et al., 2013)
	MW-03	2011	2106	~400	n/n	n/n	n/n	n/n				@1096m	@2070m	(Mbia 2014)
	MW-04	2011	2118	390	140	During flow testing		n/n	20", 94lb/ft, @81m		13 3/8", 55lb/ft @401m	9 5/8", 47lb/ft @1106m	7", 26lb/ft @2097m	(Mbia 2014) (Kipyego et al., 2013)
	MW-06 (MW-05)	2011	2203	325	n/n	n/n	n/n	n/n	20" @80m		13 3/8", 55lb/ft, 68lb/ft @409m	9 5/8 @1001m	7", 26lb/ft @2171m	(Mbia 2014) (Mibei 2012) (Kipyego et al., 2013)
Greece	*Nisyros-1*	1982	1816	>400	n/n	Wellhead using wax strips		Casing collapse	18 5/8" H40 @111m	-	13 3/8" J55, 55lb/ft BTR @414m	9 5/8" J55, 40 lb/ft, BTR @1342m	7" J55, API, 23 lb/ft @1267-1811m (slotted liner)	(Geotermica Italiana 1983, 1984)

The Sasso-22 exploration well in the Larderello field was completed in 1980 to the final depth of 4094 m. It experienced total loss of circulation from a depth of 608 m onwards, mainly due to numerous large and unsealable fractures and cavities. The rock formations drilled were extremely hard and nonhomogenous making drilling significantly difficult. A lack of drilling fluid returns forced the drilling team to use water with viscous plugs and implementing a less stiff drill string without stabilizers in order to prevent drill bit blocking during operations. This phenomenon resulted in significant difficulties in keeping the well straight. The main problems occurred below 3000 m due to the breakage of the steel drill pipes, possibly related to high temperatures and the highly corrosive nature of reservoir fluids. The primary cementing operation of the 9 5/8" production casing could not be achieved with a stinger string and had to be performed through casing perforations using squeezing techniques. Due to extremely high well temperatures reaching approximately 380 °C at depth of 3970 m, measured using wire-line logging, explosives or hydraulic fishing tools such as jars could not be used. Pumping cold water into the well proved to be efficient and helped to free the drill string. Side-tracking with cement plugs was attempted in order to continue drilling; however, cement could not be placed at the bottom of the well for centring the whipstock equipment. The main reason for the mentioned failures can be explained by the extremely high and uncontrollable reservoir temperatures. After three side-track attempts, the 9 5/8" production casing was in very poor condition and a decision was made to abandon the well soon after drilling operations ceased (Bertini 1980). Further analysis has shown that stress corrosion of casing material was aggravated with the use of steam condensates from a geothermal plant as a drilling fluid (Baron & Ungemach, 1980).

The San Vito-1 well was drilled in 1980 without any major challenges up to 2000 m depth due to the experience already gained from the other three high-temperature drilling projects in the Mofete field. The first fishing job at 2330 m resulted in some parts of the equipment being left inside the wellbore. The well was side-tracked just below the 9 5/8" production casing. Mud gelling and coagulation was experienced at 2488 m leading to stuck pipe events. An attempt of freeing the drill string with explosive materials failed due to high temperatures decomposing the explosive charges. Another attempt of side-tracking the well with coil tubing also failed and another 'fish' was left inside the hole. A back-off fishing procedure proved to be successful at 2013 m; however around 400 m of the drill string was left at the well bottom. Drilling was later continued to 3045 m and completed at the same depth with a slotted liner pipe. At 2500 m, only the melting of zinc samples was successful in registering well temperatures of about 419 °C. Production tests were attempted; however, the well showed a rapid increase of temperature at the wellhead, which was not rated for temperatures in excess of 300 °C. The San Vito-1 well was eventually killed (Baron & Ungemach, 1980). Later analysis from purge test results proved that reservoir fluid from the San Vito-1 well had a pH level of 3.2 (De Vito et al., 1989) proving an aggressive downhole environment.

The Venelle-2 well is a directional exploratory well re-drilled from one of the existing dry wells with a total depth of 2200 m and reaching temperatures of approximately 350 °C, within the Lardarello Geothermal field in southern Tuscany in the close proximity to the San Pompeo 2 well. The spudding operation began in late August of 2017. The main aim of the project was to drill into the 'K-horizon' (i.e., an important seismic marker discovered in the past deep drilling ventures in the area) located at depths of around 3000 m and reach supercritical geothermal resources. No production plans were made. During drilling operations, problems with partial and total circulation losses were experienced.

One of the main challenges during drilling of the Venelle-2 well was unexpectedly high pressures, encountered before reaching the target depths, which caused blow-out and eruption of tourmaline-quartz breccia and vein fragments. During cementing of a 7" casing section, unexpected fire occurred around the well site and cementing was interrupted causing failure of casing equipment and slurry entry to the casing. The logging campaign performed after cementing operations proved large voids in the cement sheath. The non-cemented sections at depth of 1205 m were cut off, while partially cemented sections between depths of 1205 and 1409 m were milled. Serious problems occurred during circulation stops with high-density drilling fluid of 1500 kg/m^3, which increased significantly wellhead pressure and caused problems while implementing standard well control procedures. The first stuck pipe incident occurred at a depth of 2695 m, which was attempted to release using firstly jarring and pulling up the drill string assembly and later by the decrease of drilling fluid density to 1350 kg/m^3. Problems with stuck pipe and circulation losses persisted and the well was eventually displaced with water in order to decrease well pressure and drilling fluid losses. Lower fluid pressures emphasized the need for reassessing well control practises and methods of circulation loss reduction using various squeezing and clogging techniques, which all of them proved to be unsuccessful. Challenges also occurred with setting up a swellable packer at greater depths in order to perform leak-off tests. Registering reliable temperature measurement was a serious issue in the Venelle-2 venture, where multiple temperature logging tools and methods were exercised at various drilling depths. Static formation temperatures of 504 °C at a depth of 2815 m and between 507 °C and 517 °C at a depth of 2894 m were established from available logging tools. The Venelle-2 well is currently temporarily abandoned with multiple cement plugs (Bertani et al., 2018).

Japan

The WD-1A exploration drilling project in the Kakkonda geothermal field from 1994 planned to reach a target depth of 4000 m. At depth of around 3450 m, problems with deterioration of drilling fluid properties evolved. This was caused mainly due to the rapidly increasing temperature gradient. Additionally, high contents of CO_2 and H_2S were registered in the drilling fluid returns. Higher density fluid was needed to control the harmful gases. Unfortunately, higher temperatures prevented further drilling and operations terminated at 3729 m, due to safety concerns. The well was eventually completed to 2546 m with 1183 m of open hole section. The maximum measured temperature using melting alloys was approximately 500 °C at depths below 3500 m. Full logging scheme was performed, after which the well was plugged at 2400 m with plans for future re-drilling and side-tracking (Saito et al., 1988).

Kenya

No sufficient data were found regarding well failures in geothermal wells of the Menegai geothermal field. The main challenges experienced during drilling of high-temperature wells in that area were incidents of stuck pipe between well depths of 2100 and 2200 m, where magma was encountered. Drilling of the MW-01 well was performed with partial and total circulation losses. The drill string got stuck at the end of drilling at 2206 m (Makuk 2013; Mbia 2014). During drilling the MW-03 well, a similar situation occurred at depths of 1187 and 2112 m. The well MW-04 yielded cuttings of freshly quenched volcanic glass at a depth of 2080 m. Drilling close to this magma resulted in problems such as stuck pipe at 2117 m and the drill bit damages, due to extremely high temperatures.

After unsuccessful fishing operations, around 20 m of bottom hole assembly, composed of a drill bit, sub, stabilizer, and two drill collars was abandoned inside the well. The completion was carried out with a slotted liner above the 'fish'. At final depth, rather low permeability values were encountered. Only intermittent and partial losses were experienced at the deepest well sections and no serious circulation loss problems were encountered (Mbia 2014). The MW-06 well (also called MW-05) yielded freshly quenched volcanic glassy cuttings at a depth of 2172 m. Drilling in the close vicinity to magma resulted in challenges such as stuck pipe at 2203 m. Similarly, as in MW-04, the bottom hole assembly with the length of 21 m, composed of a drill bit, sub and two drill collars was left in the wellbore and the borehole was completed with a slotted liner above the 'fish' (Makuk 2013; Mibei 2012).

Mexico

The H-43 well (Figure 5) is acid and superheated well, drilled between 2007 and 2008, in the north-western part of the Los Humeros geothermal field located at the eastern edge of the Trans-Mexican volcanic belt. This well was drilled with bentonitic drilling fluid, which masked potentially permeable zones. After washing operations, permeability was observed at a depth of 1890 m (Luviano et al., 2015). The maximum ambient well temperature measured using wire-line in the well amounted to approximately 395 °C (Pulido 2008). The H-43 well was producing superheated steam with the presence of the gaseous HCl and H_3BO_3 hostile to the mechanical infrastructure. The wellhead temperatures amounted up to 285 °C with pressures of approximately 40 bars (Gutiérrez-Negrín & Viggiano Guerra, 1990). In order to enable safe fluid production, the well was attempted to be produced under superheated conditions, so HCl would remain in dry conditions, preventing corrosion of downhole as well as surface equipment. Other challenges included erosion from powerful superheated steam and extensive precipitation (Diez et al., 2015). Similar conditions as in the H-43 well were encountered in at least seven wells drilled in the field throughout the 1980s (Castro 1996), which were eventually abandoned due to the corrosion of the mechanical construction of the well resulting from the hostile geothermal brines with a presence of gaseous HCl (Diez et al., 2015).

Figure 5: The wellhead of the abandoned H-43 well in the Los Humeros geothermal field (photo: Michal Kruszewski).

USA

The Wilson no. 1 is a wildcat well drilled to a final depth of 3672 m in 1981 at the Geysers geothermal field. At the end of drilling operations, steam entry was registered near the well bottom with pressures rising up to 94 bars and high amounts of harmful gases such as CO_2 and H_2S. A casing collapse was registered in two places in an interval between depths of 1163 and 1166 m and between 1837 and 1877 m. Additionally, incidents of a stuck pipe occurred and fishing operations were necessary. The maximum temperature estimated using fluid inclusions from a depth of 2980 m was approximately 400 °C. The well was eventually plugged with cement plugs and abandoned (DOGGR online well records 1982).

During drilling the KS-13 geothermal well in 2005 at the Puna geothermal field in the Kilauea Lower East Rift Zone in Hawaii, magma was unexpectedly intersected at depth of 2488 m causing an increase in torque values, and around 8 m of well loss. Many attempts to clean the borehole made only insignificant progress. Several kilograms of glassy cuttings were circulated out of the hole indicating penetration into the dacite magma. During reaming operations, the drill string became stuck at 2253 m and the well had to be abandoned due to the low probability of successful recovery. Unfortunately, direct well temperature and pressure measurements are not available and only the temperature of dacite magma of approximately 1050 °C is known (Spielman et al., 2006). The well served as a primary injector at the Puna geothermal field with a wellhead pressure of approximately 29 bars (Teplow et al., 2009) with a perforated liner pipe at 2124 m until it was overwhelmed by basalt lava, which erupted from the east Kilauea rift zone in May-June 2018.

Very little information is available from the IID-14 geothermal well drilled to a final depth of 2073 m and experiencing well temperatures of 390 °C (measured using wire-line logging tool at the well bottom) in the Salton Sea geothermal field. The driller reports stated that the well was uncontrollable with fresh water as a killing fluid (DOGGR online well records 1990).

1.4 Technology improvements

To allow for safe fluid production and problem-free drilling into the supercritical geothermal resources improvements of currently used technologies for drilling and well completion, adhered from the petroleum industry, are necessary. This section is divided into five subsections, i.e., drilling technology, drilling fluids, cementing operations, wellhead and casing materials, and logging technology and describes potential solutions and already made improvements in particular drilling projects in order to accommodate differences and challenges of wells investigating supercritical resources.

Drilling technology

Common to geothermal areas are hard, volcanic, abrasive, nonhomogeneous and heavily fractured rock formations which are prone to circulation loss, increased tortuosity, heavy dog legs, high tool wear and low rates of penetration. Conventional drilling tools such as tri-cone tungsten carbide insert drill bits have proven performance to approximately 180 °C, whereas directional drilling systems to temperatures up to 225 °C (Stefánsson et al., 2018), which is not sufficient for drilling into a supercritical resource. With conventional mechanical drilling technologies, penetration rates between

1 and 6 m/h are obtained, meaning that rock breaking and removal should be greatly improved in order to reduce the cost of deep drilling. Developing technologies such as metal-to-metal sealed drill bits and directional systems, hybrid bits, mud hammers or non-contact and wear-free technologies such as laser, plasma or electro-impulse drilling might allow for much faster and problem-free drilling for supercritical resources.

Extreme temperatures of circulating drilling fluids promote damages to any elastomer parts within downhole drilling and completion equipment. This eliminates the possibility of using most types of cementing, directional drilling equipment and conventional drill bit technology. During the Venelle-2 drilling campaign, a special type of PDC bit without any elastomer parts was used. This kind of 'all metallic' bits is able to operate under extreme temperature conditions. The above-mentioned drill bit technology obtained good results in terms of drilling progress and durability (Bertani et al., 2018). In the IDDP-2 drilling campaign, high-temperature tri-cone rotary drill bits and a hybrid drill bit rated for drilling fluid circulation temperatures of up to 300 °C with a specially designed high-temperature grease and metal-to-metal seals were used for operations. Both proved to function without major problems and provided sufficient penetration rates and bit life (Stefánsson et al., 2018; Chatterjee et al., 2015). Figure 6 presents a state of high-temperature drill bit parts, such as cones and bearings, after exposure to extreme temperatures in the IDDP-2 well.

Figure 6: Cones and bearing from high-temperature tri-cone roller cone drill bits used during drilling of the IDDP-2 well in the Reykjanes geothermal field in Iceland (Stefánsson et al., 2018).

During the IDDP-2 venture, together with temperature-resistant drill bits, a prototype of an elastomer-free directional drilling system with metal-to-metal seals, intended for EGS application with an aggressive fluid environment and high-temperature downhole conditions (up to 300 °C), was implemented (Chatterjee et al., 2015). The evaluation made after consecutive bit runs with the mentioned metal-to-metal directional drilling system, proved wear of rotor and stator; however, the power section was still operational and provided torque values according to manufacturer's specifications (Stefánsson et al., 2018). In general, the prototype of a directional system for geothermal wells up to 300 °C proved to work successfully during the IDDP-2 drilling operations (Friðleifsson & Elders, 2007; Friðleifsson et al., 2017).

New wear-free and contact-less drilling technologies are being currently developed at various institutions around the world. The thermal drilling methods include flame, plasma, spallation, laser, and quasi-thermal electro-impulse drilling technology. Thermal energy is used to weaken the hard rock and create spalls. Subsequently, the spalls with weakened rock are being later mechanically crushed and circulated out of the hole. Efforts within different thermal drilling technologies are ongoing in research institutions in Germany, Slovakia, and Switzerland. Another group of new technologies includes fluid-assisted drilling with high-pressure water jets. This technology is being currently researched in Germany and Austria.

Additionally, to the uncertain behavior of drilling fluid under extremely high temperatures, one of the main problems during drilling exploration wells is uncertainties related to pore and fracture pressures and potential over-pressurized zones. This problem was resolved in the Venelle-2 campaign by using Managed Pressure Drilling (MPD) system with a rotating circulation device (RDC) and Coriolis's flow meter, which is used often in depleted oil and gas reservoirs with severe circulation losses (Bertani et al., 2018). MPD systems allow maintaining well pressures slightly higher than the pore pressure, which might be a potential solution for maintaining constant downhole pressures in high-enthalpy geothermal boreholes, preventing differential sticking and allowing for much safer and more efficient drilling in severe circulation loss zones. Unfortunately, MPD systems cannot guarantee well control but rather, enable to provide constant monitoring of bottom hole pressures and flow rates. This helps to evaluate, in a real-time, variation of downhole conditions and keep the downhole pressure balance within a certain range. Installed Coriolis flow meter is able to detect any difference between flow in and out, whereas RCD choke valves are controlled, and surface back pressure is being regulated.

Drilling fluids

The main task of drilling fluid during geothermal drilling is to maintain the stability of a wellbore, provide pressure, enable cooling of the downhole environment and drilling equipment and clean the borehole from cuttings. Commonly used bentonitic drilling fluid after exposure to temperatures in the range between 150 and 200 °C (Otte et al., 1990) experiences a sharp increase in the viscosity which results in stuck pipe incidents. Bentonitic drilling fluids are preferred only for uppermost well sections, where formation collapse is expected and where temperature gradients are not as high. Commonly used polymer additives, available at the market today, are limited to circulation temperatures of approximately 90 °C (personal communication with Alexander Buchner). One of the main concerns of drilling, especially in over-pressurized zones, is exposing the drilling fluid to high temperatures, especially during long periods of drilling stoppage, and simultaneously degrading its properties. In projects such as the IDDP-2, constant total losses throughout drilling operations and highly fractured rock formations (Friðleifsson & Elders, 2017; Friðleifsson et al., 2017), resolved the problems connected to the degradation of drilling fluid properties and hole cleaning, as only clean water with polymer pills were used as drilling fluid and all created cuttings were lost in the heavily fractured geothermal reservoir. This phenomenon enabled reaching depths of nearly 4700 m. Different conditions were encountered during the drilling of the Venelle-2 well, which resulted in the usage of a water-based drilling fluid system with ilmenite and sepiolite as drilling suspending agents in order to resist high circulating temperatures and eliminate the risk of sagging. The selection of the

drilling fluid in the Venelle-2 well proved to be successful but, caused challenges during implementing standard well control procedures (Bertani et al., 2018). Improvements are needed for drilling fluids being able to maintain their properties at much higher temperatures as well as aid cleaning operations, providing good cooling capabilities and above that being environmentally friendly and biodegradable. Authors do not know about any currently undergoing research for thermally stable drilling fluids specially designed for supercritical geothermal resources.

Cementing operations

One of the crucial operations during drilling wells exploring supercritical resources is the primary cementing operation. Cement blends have to not only withstand high-temperature gradients during placement, drilling, and fluid production but also resist cyclic loading during situations such as well stimulation, production kick-off or an undesirable event of well quenching with cold water. The conventional cement mixture based on Portland cement G or H class with the addition of between 35 and 40 % of silica flour has a proven performance in conventional geothermal wells (Kosinowski & Teodoriu, 2012), where temperatures of produced fluids are below 350 °C. The Ordinary Portland Cement (OPC) experiences strength retrogression at temperature of 110 °C, after which a rapid decrease of compressive strength and chemical resistance and increase in permeability is seen. To provide good thermal as well as corrosion resistance, improved cement mixtures are necessary. These blends must ensure higher ductility of hardened cement and might include non-Portland mixtures such as geopolymers or calcium phosphate sealing systems, lower-density cement blends (e.g., foam cement) which have proven higher cement ductility and lower probability of rock fracturing during cementing operations. Another option includes adding plasticizers such as liquid latex to the conventional cement mixtures in order to create a more ductile sealing system. The Venelle-2 well can be regarded as successful use of non-Portland cement blend in geothermal well exploring supercritical resources. The cement mixture, designed for boreholes experiencing well temperatures in excess of 450 °C, was used for all 7” sections of the well and also for the temporary abandonment job and up to now, there have been no registered problems related to the cement job quality (Bertani et al., 2018).

Not only cement mixtures but also improvements of the cement placement method for primary as well as remedial cementing jobs are necessary. Stage cementing methods do not satisfy conditions of wells exploring supercritical resources, which are drilled very often in zones of partial to total losses of drilling fluid and in extremely high thermal gradients. The most suitable cementing method has to allow for continuous cementing to achieve full sealing of any existing and newly created fractures during cementing and ensure a good bond between casing and rock formations. It is usual to pump much more excess cement in a high-temperature geothermal well than it is required for a petroleum or a natural gas well. Common cementing procedures include stage, inner string, reverse circulation, tie-back, lightweight cementing and annulus packer method, which are presented in Table 2 together with their advantages and disadvantages. In recently drilled high-temperature wells, where cementing jobs at greater depths, possibly in loss circulation zones, are needed, the reverse circulation cementing method is being more commonly applied (e.g., the IDDP-1 and IDDP-2 wells in Iceland or the Habanero-4 well in Australia) (Friðleifsson & Elders, 2017; Friðleifsson et al., 2017).

Table 2: Review of common cement placement methods in geothermal wells (Table contains results from Ingason et al. (2015) and authors' state of knowledge).

Method		Advantages	Disadvantages
Stage cementing	Single-stage	Suitable once expected cement column pressure is not excessively high; lower possibility of casing collapse; method can be used as a back-up for other cementing methods	Not preferred when circulation losses occur; volume of cement mixture cannot be flexibly adjusted; continuous cementing is not allowed; long operation time; the possibility of premature cement setting; applicable only when selective intervals are to be cemented or require different cement composition
	Multi-stage		
Inner string (stinger method)		Advisable for wider casing sections; smaller cement contamination and waste; decreased displacement time; continuous cementing possible	Long tripping time of cementing string; possible failure of stage collars due to temperature conditions; potential hole packing off; possible fracturing and drilling kicks propagation; possible cement residues inside the work string and premature cement setting
Reverse circulation		Greatly reduced bottom hole pressures; reduced or eliminated need for cement retarders; lower costs of consumables and secondary cementing jobs; not all cement slurry is exposed to high temperatures; increase early cement compressive strength; decrease pumping and cement setting time; lower hydraulic horsepower of pumps required; lower cement waste; allows for continuous pumping	Cement job relies on the quality of the radioactive tracers or other dyeing products; possibly long residues of hardened cement inside the casing and at the well bottom; the uncertainty of cement reaching the casing shoe; complex cementing procedures; specialized simulation software and need for cementing specialists; unconventional and custom made cementing tools necessary; long-term effects in geothermal wells are not known
Tie-back		Easy job execution; no elastomer and temperature-sensitive parts; can be used for casing repair	Possible separation from the liner pipe; problems with placing due to debris from previous cementing jobs; additional tubing costs; possible collapse due to water pockets
Lightweight cement		Reduced pressures, fluid loss, and formation fracturing; higher compressive strengths and decreased permeability of cement; good gas migration protection; better protection against cyclic loads	High market price; additional rig equipment needed; complex cementing procedure; long term-effects in geothermal wells are not known

Cementing through annulus packer	May be positioned above loss zone to prevent migration of cement into the loss zone; easily implemented into the conventional drill string; can be activated from the surface once needed	Include elastomer parts which might fail under high temperatures; packer failure and leaking

Results of various research on cement blends in geothermal and petroleum wells proved the inadequacy of selecting the wellbore cement blends based solely on the compressive strength requirement of minimum 69 bars and permeability of at least 0.1 mD throughout exposure of 12 months to the downhole environment (API Task Group 1985). It was proven that even high compressive strengths of cement do not guarantee zonal insolation (Philippacopoulos & Brendt, 2008). Such studies have emphasized the influence on wellbore cement stresses of elastic properties of cement and rock formations such as Poisson's ratio, Young's modulus but also thickness of casing and cement as well as applied wellbore, far-field stresses, and temperature. Cement sheaths were so far regarded as a decoupled system. This is a rather simplified assumption and is not sufficient for the extreme condition of geothermal wells exploring supercritical resources, drilled in tectonically active regions with extremely high temperature and pressure gradients. For future deep drilling ventures, it is needed to look at a wellbore cement as a coupled system together with the influence of casing and rock formations. For a proper cement design, it is needed to assess an influence of stresses imposed on cement sheaths throughout the well's lifecycle (i.e. drilling, maintenance, production kick-off, fluid production), as well as in situ stresses and temperature effects. Only such detailed analysis will help to select the proper cement design and predicted cement sheaths stresses for a particular high-enthalpy geothermal field (Teodoriu 2015).

Wellhead and casing materials

Casing materials used in the geothermal industry have not changed for decades and involve either conventional API K-55 or in some cases L-80 steel grades. New inexpensive materials, that are corrosion-resistant and able to withstand high thermally induced static and cyclic loads, are of high interest in the high-enthalpy geothermal industry (Kaldal et al., 2015; 2016). Some of the potential materials which might possibly be used in wells with temperature conditions above critical include stainless steel, nickel-based alloys, titanium steels and composite metallic materials (Þorbjörnsson et al., 2015). These are, however, rather expensive and will put an immense load on the investment costs of the project. Another interesting concept is the method of cladding the casing strings with corrosion-resistant layers. Such technique is already being used in the wellhead assembly parts of wells such as the IDDP-1 and 2 (Þórhallsson et al., 2014, Friðleifsson & Elders, 2017; Friðleifsson et al., 2017). Cladding might improve the corrosion resistance of the conventional steel grades used in the geothermal industry and decrease the price relative to strings being made exclusively from expensive corrosion-resistant materials such as titanium. The main scope of the newly kick-started Geo-Coat[5] international project is to develop specialized corrosion and erosion resistant coatings for a variety of geothermal infrastructure components including casing strings, based on high entropy alloys as well

[5] http://www.geo-coat.eu/

as ceramic and metal mixtures to ensure the required bond strength, hardness, chemical resistance and density for the challenging geothermal applications.

The casing string design has to follow the assumption of extremely high temperatures and highly corrosive and hostile, especially to the mechanical infrastructure, geothermal fluids, often with high concentrations of H_2S, which might potentially lead to sulfide stress corrosion. To avoid casing failures, selection of casing strings directly exposed to the reservoir fluids (most commonly a 7" liner pipe and a 9 5/8" production casing) should be limited to casing materials designed for sour conditions. These steel grades include for instance API L-80 and T-95. In recent years, improved casing material such as TN80-3%Cr with lower corrosion rates is being employed for production casing string and liner pipe in the Los Humeros geothermal field due to the influence of hostile geothermal fluids from greater depths (Diez et al., 2015). The TN125SS casing material from the Venelle-2 campaign was selected, due to its elastic behavior with the compression load, which is the governing load. Although TN125SS is not designed especially for sour conditions, it could be used in the presence of H_2S with reservoir temperatures higher than 80 °C (Bertani et al., 2018).

Similarly, to casing material, casing connections have to withstand high thermally induced loads. Due to extremely high thermally induced cyclic stresses, it is believed that both conventional API buttress and premium casing couplings will experience failure in wells investigating supercritical resources. Extensive research is currently being carried out within the frameworks of the GeoWell and DEEPEGS project focused on the development of flexible couplings especially for high-enthalpy geothermal wells (Kaldal et al., 2016). This new solution will allow for axial movement of casing strings (as bends are not possible in a vertical wellbore) to avoid coupling rupture due to periods of heating (thermal expansion) and cooling (high tensile forces due to contraction of steel) during maintenance work and should avoid generating stresses above the yield strength of the casing material and reducing the likelihood of casing collapse. During running casing, couplings will be in open mode. While heating up, the casing material will expand allowing for each coupling to expand freely downwards via a slip-joint and closing the system before reaching the expected temperatures, with enough residual axial force to seal the connection.

To accommodate extremely high temperatures and seldom corrosive and hostile reservoir fluids, the wellhead assembly has to be diligently selected. The choice should be a compromise between wellhead quality, cost, and safety requirements. All wellhead implemented into geothermal wells has to follow API and ASME regulations. The wellheads used for both IDDP projects were ANSI class 1500 master valves with ANSI class 2500 flanges, whereas the wellhead employed for the recent Venelle-2 project was API class 10,000 rating (Bertani et al., 2018; Friðleifsson & Elders, 2017; Friðleifsson et al., 2017). In the Venelle-2 well, the base flange was realized with high corrosion resistance material. In both mentioned projects, steel cladding was realized on some parts of the surface valves and spools potentially exposed to aggressive reservoir fluids.

Logging technology

One of the most important parameters obtained from any geothermal well are temperature and pressure values. Currently, available tools allow recording temperatures with a maximum of 350 °C and 4 h of operation time. A reliable system of temperature recording at extreme temperatures in a

geothermal well was, however, yet not developed. As of today, several research projects focused on developing logging technologies for wells with extreme temperatures. One of these projects, HITI (High-Temperature Instruments for supercritical geothermal reservoir characterization and exploitation) developed a temperature logging tool for well conditions reaching the critical point of pure water (Ásmundsson et al., 2014). Another project was initiated during the Venelle-2 drilling venture in order to develop a temperature and pressure logging tool being able to withstand a temperature of 450 °C, which is much lower than temperatures actually being recorded in the Venelle-2 well, and exposure to the operation time of minimum of 6 h. The design of the mentioned tool is based on logging to an internal memory system and is powered by batteries resistant to high temperatures. Metal seals used in the tool are rated for 650 °C and measurement accuracy is 5 °C and 0.5 bars (Bertani et al., 2018).

Additional temperature measurements were installed during the IDDP-2 drilling campaign on the outside of the production casing string during running in operations. Installed at various depths between 341 and 2641 m, eight thermocouples, and a fiber optic cable were expected to enable continuously measure strain, acoustic noise and record temperatures during drilling and fluid production as well as to evaluate the quality of casing cementing operations. Thermocouples installed in the IDDP-2 well ceased to transmit temperature data after some time, even though casing was not exposed to temperatures higher than 100 °C. The condition of the fiber optic cable is yet not known, as it will be used after the IDDP-2 well is heated up (Friðleifsson & Elders, 2017; Friðleifsson et al., 2017).

Temperature measurement methods in wells exploring supercritical resources vary from well to well, with direct temperature measurements such as wire-line logging to more indirect methods such as fluid inclusions, melting materials or estimating magma temperature. In some cases, temperature measurements were carried out inside the well, not necessarily at well bottom, during drilling fluid circulation and in other, directly at the wellhead assembly during fluid production. Information about pressure conditions was unfortunately not accessible for all of the studied wells. Future supercritical projects might find it rather difficult to assess thermal recovery data from the wells exceeding the critical point of reservoir fluids in order to establish undisturbed pressure and temperature conditions of the geothermal reservoir for further modeling activities. As experience from past campaigns has proven, such data will be normally assessed using a variety of different measuring techniques and will provide a range of temperature and pressure values.

1.5 Conclusions

Defining failure modes for studied wells proved to be difficult, due to the lack of detailed data, published well reports and literature available and authors had to base their knowledge on a small and limited amount of published data. From the 20 drilling projects presented in Table 1, drilled in or close to supercritical conditions, failure modes are known only for a few wells. In most cases, failure of the geothermal well was caused by excessively high thermally induced stresses exerted upon the casing string and couplings during operations such as well quenching or production kick-off causing casing collapse and/or connections rupture. Casing collapse in some cases was also propagated by bad cementing jobs commonly executed in zones of partial or total circulation loss. In few wells, blow-out or near-blow-out conditions were encountered, which in most cases precluded further

drilling due to safety concerns. In older wells, not aimed to penetrate the supercritical resource, such as KJ-39, NJ-11, KS-13 or San Vito-1, the well design was not rated for such extreme temperature and pressure conditions and well completion was finalized at much shallower depths. Some of the mentioned wells, after reconstruction work, serve today as injection wells. In other wells, investigation of deeper supercritical resources had to be halted due to safety reasons of ejection of hostile gases, such as H_2S, which might have promoted damages to the mechanical infrastructure and cause health and life danger. The heavy precipitation, corrosion, and erosion due to high flow rates of hostile and oftentimes hypersaline geothermal brines are also noted as serious issues, especially during fluid production and well testing.

Recently undertaken European initiatives investigating supercritical geothermal resources greatly improved state of knowledge in regard to the drilling technology, drilling fluids, cementing operations, wellhead and casing materials and logging technology for high-temperature wells going beyond what is considered currently as a standard in the geothermal industry. It was with their help that the development of new equipment and downhole tools was possible, and areas of potential improvement were emphasized. It would be beneficial for mitigating challenges and improving the learning curve for wells investigating high-temperature geothermal reservoirs, to establish a dialog with the petroleum industry where scientists and engineers can cross-fertilize experiences and ideas, which could be valuable for upcoming supercritical projects. The biggest potential technology transfer could be possible for thermally enhanced oil recovery industry researching steam-assisted gravity drainage and cyclic steam injection methods.

References

API Task Group on Cements for Geothermal Wells, API Work Group reports field tests of geothermal cements, Oil and Gas Journal 93–97, 1985.

Ármannsson H., Fridriksson T., Gudfinnsson H.G., Ólafsson M., Óskarsson F., Thorbjörnsson D., The chemistry of the IDDP-1 well fluids in relation to the geochemistry of the Krafla geothermal system, Geothermics 49, 66–75, 2014.

Armenta M.C.F., Montez R.M., Drilling of bilateral wells: analysis and selection of wells in the Los Humeros Geothermal Field, Geotermia, Vol. 23, No.1, Enero-Junio de 2010.

Árnadóttir S., Mortensen A.K., Egilson T., Gautason B., Ingimarsdóttir A., Massiot C., Jónsson R.B., Sveinbjörnsson S., Tryggvason H.H., Krafla – Leirbotnar Hola KJ-39, ÍSOR-2009/059 Verknr. 521027, December 2009.

Asanuma H., Tsuchiya N., Muraoka H., Ito H., Japan Beyond-Brittle Project: Development of EGS Beyond Brittle-Ductile Transition, Proceedings World Geothermal Congress 2015 Melbourne, Australia, 19-25 April 2015.

Baron G., Ungemach P., European Geothermal Drilling Experience Problem Areas and Case Studies, Commission of The European Communities, Belgium, 1980.

Bertani R., Büsing H., Buske S., Dini A., Hjelstuen M., Luchini M., Manzella A., Nybo R., Rabbel W., Serniotti L., The First Results of the DESCRAMBLE Project, PROCEEDINGS, 43rd Workshop on Geothermal Reservoir Engineering Stanford University, Stanford, California, February 2018.

Bertini C., Giovannoni A., Stefani G.C., Deep Exploration in Larderello Field: Sasso 22 Drilling Venture, Enel Unita Nazionale Geotermica, Pisa, Italy, Advances in European Geothermal Research, Brussels and Luxembourg 1980.

Bischoff J. L., Rosenbauer J. R., The critical point and two-phase boundary of seawater 200 – 500°C, Earth and Planetary Science Letters, 68 (1984) 172 – 180, Elsevier Science Publishers B.V., Amsterdam.

Böðvarsson G., 1961. Physical characteristics of natural heat resources in Iceland. Jökull, pp. 29-38.

Bottai A. Cigni U., Completion Techniques in Deep Geothermal Drilling, Geothermics, Vol. 14, No. 2/3, pp. 309 - 314, 1985.

Carson S. C., Geothermal Drilling Problems and Their Impact on Cost, Sandia National Laboratories, SAND82-0261C, DE82 020626.

Castro S. C., Well Repairing at The Los Humeros, Mexico, Geothermal Field, Geothermal Resources Council TRANSACTIONS, Vo. 20, September/October 1996.

Chatterjee K., Dick A., Grimmer H., Herlitzius J., Otto M., Klotzer S., Epplin D., Schroder J., Macpherson J., High-Temperature, 300 °C Directional Drilling System Including Drill Bit, Steerable Motor, and Drilling Fluid, GRC Transactions, Vol. 38, 2014.

Chiotis E., Vrellis G., Analysis of Casing Failures of Deep Geothermal Wells in Greece, Geothermics Vol. 24, No. 5/6, pp. 695-705, 1995.

Cladouhos T., Petty S., Bonneville A., Schultz A., Sorlie C.F., Super-Hot EGS and the Newberry Deep Drilling Project, Proceedings of the 43rd Workshop on Geothermal Reservoir Engineering Stanford University, Stanford, California, February 2018.

De Vito B., Belkin H.E., Barbieri M., Chelini, W., Lattanzi P., Lima A., Tolomeo L., The Campi Flegrei (Italy) geothermal system: A fluid inclusion study of the Mofete and San Vito fields, Journal of Volcanology and Geothermal Research Volume 36, Issue 4, Pages 303-326, 1989.

Diez H., Flores M., Ramirez M., Tovar R., Rosales C., Solano F., Sandoval F., Neutralization of Acid Fluids from Well H-43 (Superheated Steam), Los Humeros Geothermal Field, Mexico, Proceedings World Geothermal Congress 2015, Melbourne, Australia, 19-25 April 2015.

Einarsson K., Pálsson B., Gudmundsson A., Hólmgeirsson S., Ingason K., Matthíasson J., Hauksson T., Ármannsson H., Acid Wells in the Krafla Geothermal Field, Proceedings World Geothermal Congress 2010, Bali, Indonesia, 25-29 April 2010.

Elders W.A., Friðleifsson G.Ó., Albertsson A., Drilling into magma and the implications of the Iceland Deep Drilling Project (IDDP) for high-temperature geothermal systems worldwide, Geothermics 49, 111-118, 2014.

Elders W.A., Friðleifsson G.Ó., Investigating a Mid-Ocean Ridge Hydrothermal System on Land: the Iceland Deep Drilling Project on the Reykjanes Peninsula in SW Iceland, Proceedings World Geothermal Congress 2015, Melbourne, Australia, 19-25 April 2015.

Elders W.A., Sass J., The Salton Sea Scientific Drilling Project, Journal of Geophysical Research, Vol. 93, No. B11, Pages 12, 953-12, 968, November 10, 1988.

Friðleifsson G.Ó., Armannsson H., Gudmundsson A., Arnason K., Mortensen A.K., Palsson B., Einarsson G.M., Site Selection for the Well IDDP-1 at Krafla, Geothermics 49, 9 – 15, 2014a.

Friðleifsson G.Ó., Blischke A., R. B. Kristjánsson, Richter B., Einarsson M.G., Jónasson H., Franzson H, Sigurðsson Ó., Danielsen E. P., Jónsson S. S., Thordarson S., Þórhallsson S., Harðardóttir V., Egilson Þ., Well Report RN-17 & RN-17ST, ÍSOR-2005/007, ISBN 9979-780-26-6, July 2005.

Friðleifsson G.Ó., Elders W.A., Albertsson A., The concept of the Iceland Deep Drilling Project, Geothermics 49, 2-8, 2014b.

Friðleifsson G.Ó., Elders W.A., Successful drilling for supercritical geothermal resources at Reykjanes SW Iceland, Transactions Geothermal Resources Council, 41, 1095-1106, 2017a.

Friðleifsson G.Ó., Elders W.A., Zierenberg R.A., Stefánsson A., Fowler A.P.G., Weisenberger T.B., Harðarson B.S., Mesfin K.G., The Iceland Deep Drilling Project 4.5 km deep well, IDDP-2, in the sea-water recharged Reykjanes geothermal field in SW Iceland has successful reached its supercritical target, Scientific Drilling, no. 23, 1-12, 2017b.

Garcia J., Hartline C., Walters M., Wright M., Rutqvist J., Dobson F. R., Jeanne P., The Northwest Geysers EGS Demonstration Project, California Part 1: Characterization and reservoir response to injection, Geothermics, Volume 63, September 2016, Pages 120–138, 2016.

García-Gutiérrez, Arellano, Barragán, Espinosa-Paredes, Initial temperature field in the Los Humeros geothermal reservoir, Geofísica Internacional (2002), Vol. 41, Num. 3, pp. 303-312.

Geotermica Italiana, Nisyros 1 geothermal well. Final (unpublished) report, Pisa, 1983.

Geotermica Italiana, Nisyros 2 geothermal well. Final (unpublished) report, Pisa, 1984.

Hodson-Clarke A., Rudolf R., Bour D., Russell P., Key Factors to Successful Drilling and Completion of EGS Well in Cooper Basin, PROCEEDINGS, 41st Workshop on Geothermal Reservoir Engineering Stanford University, Stanford, California, February 22-24, SGP-TR-209, 2016.

Ingason K., Árnason A.B., Bóasson H.A., Sverrisson H., Sigurjónsson K.O., Gíslason T., IDDP-2, Well design, Proceedings World Geothermal Congress 2015, Melbourne, Australia, 19-25 April 2015.

Ingason K., Kristjansson V., Einarsson K., Design and development of the discharge system of IDDP-1, Geothermics 49, 58-65, 2014.

Kaldal G.S., Jónsson Þ.M., Pálsson H., Karlsdóttir S.N., Structural Analysis of Casings in High Temperature Geothermal Wells in Iceland, Proceedings of World Geothermal Congress 2015, Melbourne, Australia, 19-25 April 2015.

Kaldal G.S., Þorbjörnsson O. I., Thermal expansion of casings in geothermal wells and possible mitigation of resultant axial strain, European Geothermal Congress 2016, Strasbourg, France, 19-24 Sept 2016.

Karlsdottir S.N., Ragnarsdottir K.R., Thorbjornsson I.O., Einarsson A., Corrosion testing in superheated geothermal steam in Iceland, Geothermics 53 p. 281–290, 2015.

Karlsson T., Casing design for high temperature geothermal wells, Transactions of Geothermal Resource Council, 2, 355-358, 1978.

Kipyego E., O'Sullivan J., O'Sullivan M., An initial resource assessment of the Menengai caldera geothermal system using an air–water TOUGH2 model. In: Proceedings, 35th New Zealand Geothermal Workshop, Rotorua, New Zealand; 2013.

Kosinowski, C., Teodoriu, C., Study of Class G Cement Fatigue using Experimental Investigations, EAGE European Unconventional Resources Conference and Exhibition held in Vienna, Austria, 20-22 March 2012.

Lazzarotto A., Sabatelli F., Technological Developments in Deep Drilling in the Larderello Area, Proceedings World Geothermal Congress 2005, Antalya, Turkey, 24-29 April 2005

Luviano S.M., Armenta F.M., Montes R.M., Thermal Stimulation to Improve the Permeability of Geothermal Wells in Los Humeros Geothermal Field, Mexico, Proceedings World Geothermal Congress 2015, Melbourne, Australia, 19-25 April 2016.

Maruyama K., Tsuru E., Ogasawara M., Inoue Y., Peters J. E., An Experimental Study of Casing Performance Under Thermal Recovery Conditions, SPE 18776, SPE California regional meeting, Bakersfield, California, April 5 -7 1989.

Mbia K. P., Sub-Surface Geology, Petrology and Hydrothermal Alteration of Menengai Geothermal Field, Kenya, Master Thesis, United Nations University Geothermal Training Programme, Reykjavík, Iceland, ISBN 978-9979-68-339-1, ISSN 1670-7427, 2014.

Mendrinos D., Choropanitis I., Polyzou O., Karytsas C., Exploring for geothermal resources in Greece, Geothermics 39, 124–137, 2010.

Mibei G., Geology and Hydrothermal Alteration of Menengai Geothermal Field. Case Study: Wells MW-04 and MW-05, Geothermal Training Programme, Orkustofnun, Report Number 21, Reykjavik, Iceland, 2012.

Mortensen A. K., Grönvold K., Gudmundsson A., Steingrímsson B., Egilson T., Quenched Silicic Glass from Well KJ-39 in Krafla, North-Eastern Iceland, Proceedings World Geothermal Congress 2010 Bali, Indonesia, 25-29 April 2010.

New Zealand Standard: Code of practice for deep geothermal wells from 1991 (NZS 2403:1991) and recent update from 2015 (NZS 2403:2015).

Okwiri L.A., Cherutisch S., Drilling in Menengai Field – Success and Challenges, UNU-GTP, GDC and KenGen, Lake Bogoria and Lake Naivasha, Kenya, Oct. 31 – Nov. 22, 2013.

Otte C., Pye D.S., Stefanides N.J., The Applicability of Geothermal Drilling Experience to Super-Deep Drilling. In: Fuchs K., Kozlovsky Y.A., Krivtsov A.I., Zoback M.D. (eds) Super-Deep Continental Drilling and Deep Geophysical Sounding. Exploration of the Deep Continental Crust. Springer, Berlin, Heidelberg, 1990.

Pálsson B., Hólmgeirsson S., Guðmundsson A., Bóasson H. A., Ingason K., Sverrisson H., Thórhallsson S., Drilling of the well IDDP-1, Geothermics 49, 23–30, 2014

Philippacopoulos A., Berndt M., Structural analysis of geothermal well cements, Geothermics 31, 657–676, 2002.

Pulido C.D.L., Borehole Geophysics and Geology of Well H-43, Los Humeros Geothermal Field, Puebla, México, Geothermal Training Programme, Reports 2008, Number 23, Orkustofnun, Reykjavík, Iceland, 2008.

Reinsch T., Dobson P., Asanuma H., Huenges, Poletto F., Sanjuan B.: Utilizing supercritical geothermal systems: a review of past ventures and ongoing research activities, Journal Geothermal Energy, 2017.

Ross P. H., Salton Sea Scientific Drilling Project – Final Report, A Summary of Drilling and Engineering Activities and Scientific Results, The U.S. Department of Energy Geothermal Division, November 1991.

Ruggieri G., Gianelli G., Fluid inclusion data from the Carboli 11 well, Larderello geothermal field, Italy, World Geothermal Congress, Italy, pp. 1087-91, 1995.

Saito S., Sakuma S., Uchida T., Drilling Procedures, Techniques and Test Results for a Deep, 500°C Exploration Well, Kakkonda, Japan, Geothermics Vol. 27, No. 5/6, pp. 573-590, 1998.

Scott S., Driesner T., Weis P., Geologic controls on supercritical geothermal resources above magmatic intrusions, Nature Communications, Vol. 6, Article number 7837, 2015.

Spielman P., Rickard W., Teplow W., Puna Geothermal Venture, Hawaii – 2005 Drilling Program, Transactions of Geothermal Resources Council, Vol. 30, 2006.

Stefánsson A., Duerholt R., Schroder J., Macpherson J., Hohl C., Thomas Kruspe T., Eriksen T.J., A 300 Degree Celsius Directional Drilling System, Society of Petroleum Engineers, IADC/SPE Drilling Conference and Exhibition, 6-8 March, Fort Worth, Texas, USA, 2018.

Stefánsson A., Gílason T., Sigurdsson Ó., Friðleifsson G.Ó., The drilling of the RN15/IDDP-2 research well at Reykjanes SW Iceland. Transactions Geothermal Council, Vol 41. p. 512-520, 2017.

Steingrimsson B., Gudmundsson A., Sigvaldason H., Sigurdsson O., Gunnlaugsson E., Nesjavellir, Hola NJ-11, Borun, rannsoknir og vinnslueiginleikar, OS-86025/JHD-05, Reykjavik, April 1986.

Teodoriu C., Why and When Does Casing Fail in Geothermal Wells: A Surprising Question? Proceedings World Geothermal Congress 2015, Melbourne, Australia, 19-25 April 2015.

Teplow W., Marsh B., Hulen J., Spielman P., Kaleikini M., Fitch D., Rickard W., Dacite Melt at the Puna Geothermal Venture Wellfield Big Island of Hawaii, Transactions of Geothermal Resources Council, Vol. 33, 2009.

Þorbjörnsson O.I., Karlsdottir N.S., Einarsson A., Ragnarsdottir R.K., Materials for Geothermal Steam Utilization at Higher Temperatures and Pressures, Proceedings Word Geothermal Congress 2015, Melbourne, Australia, 19-25 April 2015.

Þórhallsson S., Bjarni Palsson B., Hólmgeirsson S., Ingason K., Matthíasson M., Bóasson H. A., Sverrisson H., Well design and drilling plans of the Iceland Deep Drilling Project (IDDP), Proceedings World Geothermal Congress 2010 Bali, Indonesia, 25-29 April 2010.

Þórhallsson S., Matthíasson M., Gíslason T., Ingason K., Pálsson B., Friðleifsson G.Ó., IDDP Feasibility report, Iceland Deep Drilling Project, PART II Drilling Technology, 2003.

Þórhallsson S., Palsson B., Holmgeirsson S., Ingason K., Matthiasson M., Boasson H.A., Sverrisson H., Well design for the Iceland Deep Drilling Project (IDDP), Geothermics 49, 16-22, 2014.

2 Determination of the In-Situ Stress Tensor of the Los Humeros Geothermal Field in Mexico

(Michal Kruszewski, Giordano Montegrossi, Francesco Parisio, Erik H. Saenger)

This work has been published in:

- *Kruszewski M., Montegrossi G., Ramirez M., Wittig V., Garcia G.A., Sanchez M., Bracke R., Wellbore Stability and Scientific Basis for Geomechanical Modeling on the Example of the Los Humeros Geothermal Field, Mexico, Geophysical Research Abstracts Vol. 21, EGU2019-PREVIEW, 2019, EGU General Assembly 2019, Vienna, Austria, 7 – 12 April 2019.*
- *Kruszewski M., Montegrossi G., Ramirez M., Wittig V., Sanchez M., Bracke R., Crustal Stress determination and wellbore stability analysis: Los Humeros geothermal field case study, Proceedings of the European Geothermal Congress 2019, Den Haag, The Netherlands, 11-14 June 2019.*

This work also relates to the manuscript by Kruszewski M., Montegrossi G., Parisio F., Saenger E. H. entitled "Determination of the In-Situ Stress State of the Los Humeros Volcanic Complex (Mexico) Based on Borehole Observations" submitted to the Rock Mechanics and Rock Engineering (Springer) journal which is currently under the review process.

2.1. Introduction

Obtaining qualitative information about the stress state in the Earth's crust is a challenging task. Typically, direct measurements of crustal stresses are not included in logging campaigns of deep geothermal wells, especially in high enthalpy reservoirs in which temperature conditions exceed the operational limits of the logging equipment. Underground rock formations are confined and remain under defined stress state. In-situ stresses are anisotropic, compressive, inhomogeneous, and increase with depth (Gidley et al., 1989). The knowledge of the direction and magnitude of vertical stress (S_V), minimum (S_{hmin}), and maximum horizontal (S_{Hmax}) stresses is important as they control the pressure required to propagate shape, vertical extent, and direction of a fracture. Within homogenous Earth, rapid and/or large stress gradient changes are not expected. The situation is however different, once cavity, i.e. a borehole, is created (Zoback 2007).

Having a comprehensive geomechanical model allows addressing a series of problems related to wellbore stability. The applied drilling fluid pressure has a major effect on the stability of the borehole during drilling. With applied fluid pressure being lower than collapse pressure, the open hole section can experience compressive failure which can lead to deformations of the wellbore wall such as borehole breakouts, wash-out's or total collapse of open hole section. Further decrease of drilling fluid pressure, below the pore pressure, can result in an undesirable event of drilling kick or blow-out. On the other hand, high drilling fluid pressure exceeding the fracture pressure can result in drilling-induced tensile fractures leading to partial or even total fluid losses (Pašić et al., 2007). The stable pressure window during drilling is thus localized between collapse and fracture pressure. Achieving such a delicate balance of pressures in relatively unknown systems or greenfields is a big challenge. Therefore, in order to aid mentioned problems and determine safe casing setting depths,

choose appropriate well completion, trajectory, and cementing strategy, solid knowledge of stress state in-situ is required (Peska et al., 1995).

The Los Humeros geothermal field (LHGF) is located at the eastern section of the Trans-Mexican Volcanic Belt (TMVB) at the border of Veracruz and Puebla states and is one of the four most productive geothermal fields in Mexico (represented with a red square in Figure 7). The eastern section of the TMVB, on which the Los Humeros caldera is located, is defined by the ENE-WSW trending major stress direction and a normal faulting stress regime (Suter 1991), as shown in Figure 7. At least three main fault systems, controlling the ascent of geothermal fluids, can be defined within the Los Humeros caldera. First, the NW-SE trending faults, limited mainly to the south of the geothermal field and shifting to NNW-SSE and later on to the N-S trending fault system. The E-W trending fault system, characteristic to the eastern side of the caldera, cut by multiple secondary oblique local WNW-striking faults (Carrasco-Nunez et al., 2015).

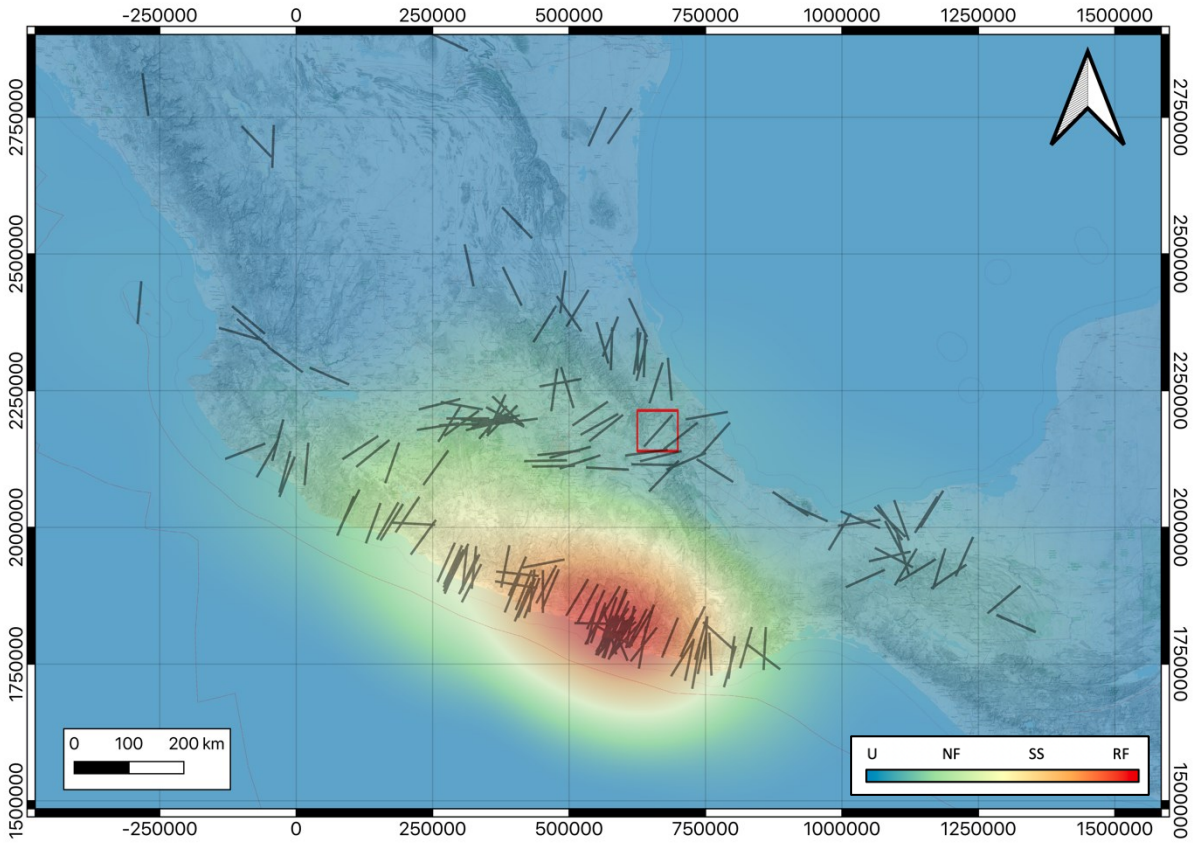

Figure 7: The stress map of Mexico; color scale indicates stress regimes with U – unknown, NF – normal faulting, SS – strike-slip faulting, and RF – reverse faulting; red square represents the location of the LHGF; black lines indicate azimuths of S_{Hmax} (map constructed based on data from Heidbach et al. 2016).

This study presents an innovative approach for the assessment of crustal stresses using non-direct stress measurements such as drilling parameters and six-arm caliper log results. The investigation was based on the results from deep drilling operations within the Los Humeros Geothermal Field. During almost 40 years of geothermal drilling in the field, issues related to wellbore instability have been observed in multiple boreholes. The results of this study provide valuable insights into the still

poorly constrained local in-situ stress state of the Los Humeros geothermal field and support the exploration of supercritical geothermal resources therein.

2.2. Methods

Vertical stress

While evaluating in-situ stresses in the reservoir it is assumed that one of the principal stresses is vertical. It is mainly by stresses generated by the gravity force are directed downwards. Assuming this, principal vertical stress can be calculated at defined well depth using the density of the particular rock formation and the gravitational acceleration constant (Zoback 2007). The vertical stress component can be easily obtained from density logs, using the equation below, or through laboratory measurements

$$S_V = \int_0^z \rho_f(z) g dz \tag{2.1}$$

where ρ_f is the density of rock formations in kg/m^3, z is depth in m, and g is gravitational acceleration in m/s^2.

Horizontal stresses

Borehole breakouts, as presented in Figure 8, are spalled symmetrical regions at each side of the borehole wall, centred at the azimuth of the minimum horizontal stresses and located perpendicular to the maximum horizontal stresses, found in any type of formation rock and the tectonic environment in which the average azimuth of the long interval section is consistent within given petroleum or geothermal field. These enlargements of the borehole wall are caused by the failure that takes place once maximum tangential wellbore stresses exceed the compressive strength of the formation rock (Zoback 1985; 2007). Laboratory studies made by Haimson & Edl (1972) have proven that borehole breakouts extend throughout the circumference of the borehole and their depth presents a clear increase in respect to the increase of confining pressure. These claims were later confirmed by Haimson & Herrick (1985), which concluded that the breakout width and depth are directly correlated to the magnitude of the minimum horizontal stresses.

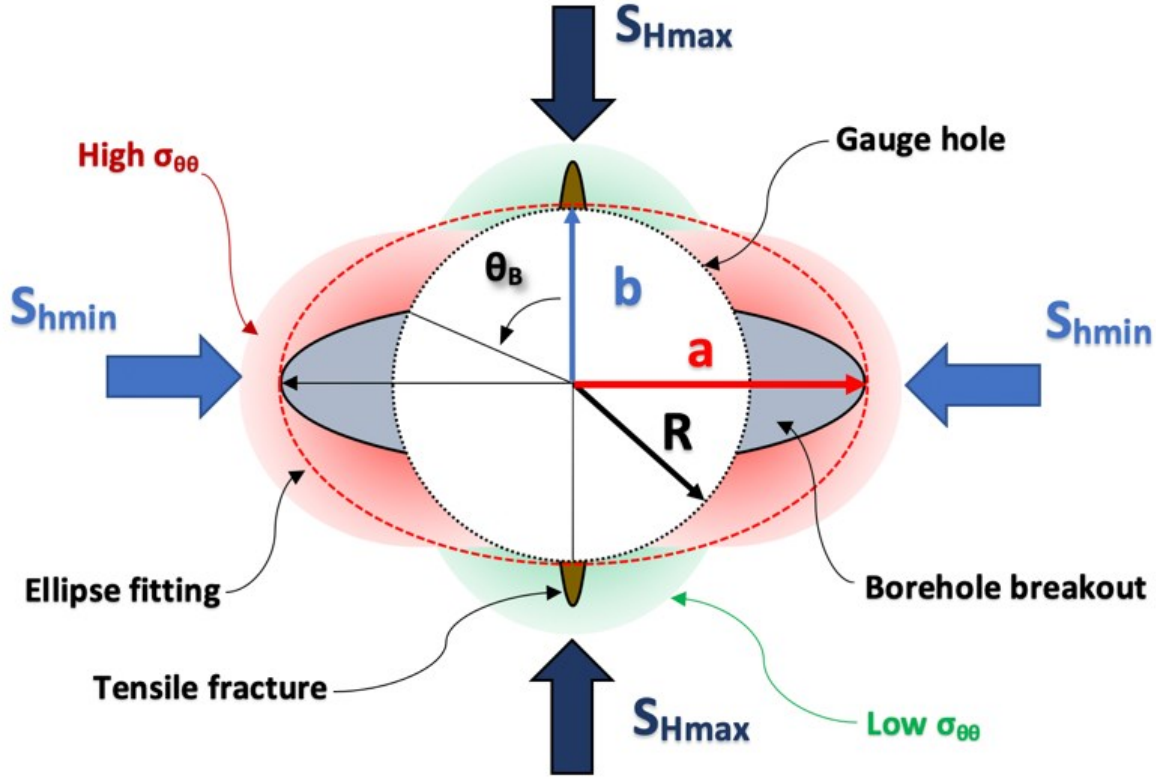

Figure 8: A schematic picture of a borehole breakout with acting minimum and maximum horizontal stress and the ellipse fitting approach (a – semi-major axis, b – semi-minor axis, R – in-gauge hole radius, θ_B – an azimuth measured from the direction of S_{Hmax}).

In order to compute orthogonal maximum and minimum open hole diameters as well as breakout orientation, the ellipse fitting method was developed. For fitting the ellipse on the mechanical six-arm caliper measurement points obtained from the H-64 well equations by Fitzgibbon (1999) were applied, whereas the best fit is based on a general conic equation. The ellipse fitting method uses the least square criterion. The resulting data is used for further investigation of minimum and maximum horizontal stresses and breakout orientation. To calculate the minimum and maximum horizontal stresses from the six-arm mechanical caliper log carried out in the H-64 well, theoretical equations Zoback (1985) were applied, where a cylindrical hole is considered in a thick, homogeneous, isotropic and elastic plate subjected to the maximum and minimum principal stresses. Assumptions made for computations of minimum and maximum horizontal stresses include no excess pressure in the wellbore and $S_{Hmax} \leq 3S_{hmin}$, which is always the case in-situ (Brace & Kohlstedt 1980; Zoback 2007). Equations developed by Zoback (1985) allowed expressing the cohesive strength of formation rocks at the point of intersection between breakout and the wellbore and at the deepest breakout point. Assuming that breakouts follow a trajectory along given cohesive strength of rock allowed assessing minimum and maximum horizontal stresses. The frictional sliding friction coefficient for the case of LHGF in a range between 0.6 and 0.85 (Byerlee 1978) was assumed.

Drilling fluid losses are the result of the applied total wellbore pressure (i.e. a sum of drilling fluid column and stand-pipe pressures), calculated using the equation below, exceeding the minimum principal stress in the open hole section, leading to its tensile failure. This assumption allows assessing

the minimum principal stress at intervals of drilling fluid loss, assuming that no natural pre-existing fractures were intersected. Calculations are carried out using drilling parameters, recorded simultaneously during the drilling process. It is worth mentioning, that the circulation loss records are commonly very inconsistent and rely often on the notes made by the drilling personnel only.

$$P_W = P_{SPP} + \rho_m g z \tag{2.2}$$

Where ρ_m is the density of drilling fluid in kg/m^3, P_{SPP} is the stand-pipe pressure in Pa. The fluid loss data from three high-temperature wells within the LHGF were considered for the analysis of minimum principal stresses from the drilling fluid loss reports.

2.3. Conclusions

We have employed the ellipse fitting method on borehole breakout shapes localised with a six-arm caliper log on an existing wellbore to determine the orientation of S_{Hmax} and predict magnitudes of the principal in-situ stresses at Los Humeros geothermal field in Mexico. Based on the data acquired within this study, we conclude that the local stress regime in the vicinity of the H-64 well is between strike-slip and reverse faulting with E-W direction of the maximum horizontal stress (Figure 9). The local in-situ stress state within the Los Humeros caldera remains strongly heterogeneous and presents high spatial discrepancies and strong variations with depth. Carrying out direct in-situ measurements and analysing greater amounts of drilling data, caliper and image logs to infer orientations and magnitudes of the principal in-situ stresses is crucial to better constrain the complex local in-situ stress state within the Los Humeros caldera and support exploration of super-hot resources. Results from this study may serve as basis for the design of drill paths for the future supercritical wells within the LHGF. We use the investigation of the crustal stresses, carried out in this chapter, for computations of cement sheath stresses and its failure carried out in Chapter 3.

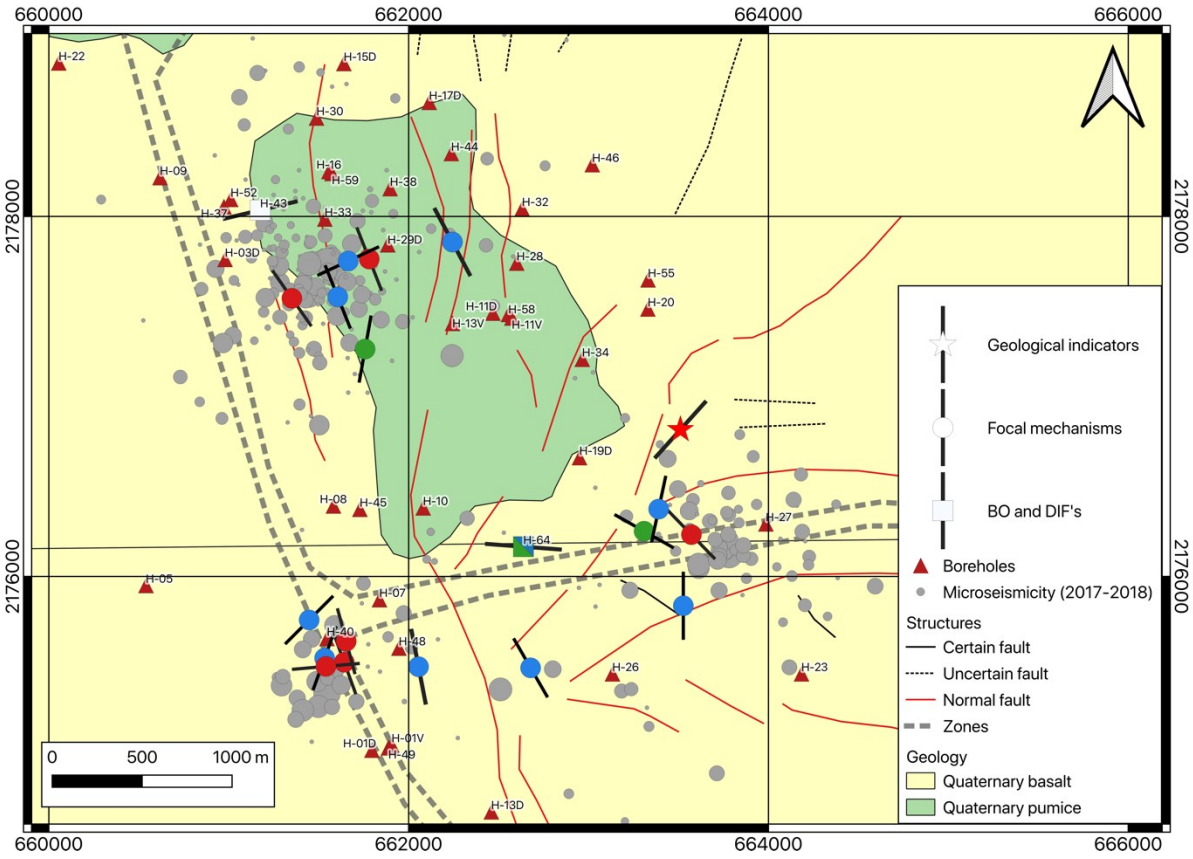

Figure 9: The map of LHGF with stress indicators from H-64 well and from studies by Heidbach et al. (2016), Lermo et al. (2016), Lorenzo-Pulido (2008), and Toledo et al. (2019); blue marker color indicates reverse faulting, green – strike-slip, red – normal faulting, and white – unknown; S_{Hmax} azimuth represented with a thick black line; microseismicity data recorded between 2017 and 2018 by Toledo et al. (2019) with dot size proportional to the earthquake magnitude.

References

Brace A.B., Kohlstedt D.L., Limits on lithospheric stress imposed by laboratory experiments, Journal of Geophysical Research, 85, 6248-6252, 1980.

Byerlee J., Friction of Rocks, Pageoph, Vol. 116, Birkhfiuser Verlag, Basel, 1978.

Carrasco-Núñez G., Arzate J., Bernal J.P., Carrera J., Cedillo F., Dávila-Harris P., Hernández J., Hurwitz S., Lermo J., Levresse G., López P., Manea V., Norini G., Santoyo E., Willcox C., A New Geothermal Exploration Program at Los Humeros Volcanic and Geothermal Field (Eastern Mexican Volcanic Belt), Proceedings World Geothermal Congress 2015, Melbourne, Australia, 19-25 April 2015.

Fitzgibbon A., Pilu M., Fisher R.B., Direct least square fitting of ellipses, IEEE Transactions on Pattern Analysis and Machine Intelligence, Vol. 21, Issue 5, 1999.

Gidley J.L., Holditch S.A., Nierode D.E., Rock Mechanics and Fracture Geometry, Recent Advances in Hydraulic Fracturing, Chapter 3, 57-63. Richardson, Texas, Monograph Series, SPE, 1989.

Haimson B.C., Edl J.N., Hydraulic fracturing of deep wells, SPE Paper No. 4061, 1972.

Haimson B.C., Herrick C., In-situ stress evaluation from borehole breakouts: experimental studies, in Proc. 26th US Symp. Rock Mech., Rapid City, Balkema, Rotterdam, 1207-1218, 1985.

Heidbach O., Rajabi M., Reiter K., Ziegler M., WSM Team, World stress map database release 2016.

Lorenzo-Pulido C.D., Borehole Geophysics and Geology of Well H-43, Los Humeros Geothermal Field, Puebla, México, Reports of Geothermal Training Programme, United Nations University, Orkustofnun, Grensásvegur 9, IS-108 Reykjavík, Iceland, Reports 2008, Number 23, 2008.

Pašić B., Gaurina-Međimurec N., Matanović D., Wellbore Instability: Causes and Consequences, UDC 622.32:622.248, Rudarsko-geološko-naftni zbornik, Vol. 19, str. 87 - 98 Zagreb, 2007.

Peska P., Zoback M.D., Compressive and tensile failure of inclined well bores and determination of in situ stress and rock strength, Journal of Geophysical Research Atmospheres, 12791, 1995.

Rodríguez H., Lermo J., Urban E., Analysis of Seismic Anisotropy in Los Humeros Geothermal Field, Puebla, Mexico, Proceedings, Thirty-Seventh Workshop on Geothermal Reservoir Engineering, Stanford University, Stanford, California, January 30 - February 1, 2012.

Suter M., State of stress and active deformation in Mexico and western Central America, The Geology of North America, Decade Map Volume 1, 1991.

Toledo Zambrano T. A., Gaucher E., Metz M., Calò M., Figueroa A., Angulo J., Jousset P., Kieling K., Saenger E., Dataset of the 6G seismic network at Los Humeros, 2019.

Zoback M.D., Moos D., Mastin L., Anderson R., Well Bore Breakouts and in Situ Stress, Journal of Geophysical Research, Vol. 90, No. B7, Pages 5523-5530, June 10, 1985.

Zoback M.D., Reservoir Geomechanics, Cambridge University Press, 2007.

3 A Wellbore Cement Sheath Damage Prediction Model with the Integration of Acoustic Wellbore Measurements and Experimental Laboratory Studies on Non-Portland Sealants

(Michal Kruszewski, Giordano Montegrossi, Marvin Glissner, Volker Wittig)

Parts of this work have been published in:

- *Kruszewski M., Ramirez M., Wittig V., Sanchez M., Bracke R., Drilling and Well Completion Challenges in the Los Humeros Geothermal Field, Mexico, GRC Transactions, Vol. 42, 2018.*
- *Kruszewski M., Montegrossi G., Ramírez Montes M., Wittig V., Gomez Garcia A., Sánchez Luviano M., Bracke R., A wellbore cement sheath damage prediction model with the integration of acoustic wellbore measurements, Geothermics 80:195-207, 2019, DOI 10.1016/j.geothermics.2019.03.007.*

This work also relates to the manuscript by Kruszewski M., Glissner M.., Hahn S., Wittig V. entitled "Alkali-activated Aluminosilicates Sealing System for Deep High-Temperature Well Applications" submitted to the Geothermics journal which is currently under the review process.

3.1. Introduction

The primary cementing operation is a crucial activity carried out during drilling any type of well. Three of the main purposes of a cementing job are to assure zonal isolation, provide mechanical support for casing strings, and protect well construction against corrosion resulting from the often-hostile reservoir fluids, throughout the well lifecycle. When one of these points is not achieved, wellbore integrity is compromised, which may lead to serious failures and, potentially to the total well abandonment. High-temperature geothermal wells proved to have an issue with providing mechanical support. Also, zonal isolation may not be a key requirement due to the extensive water circulation, common for hydrothermal systems. Such a phenomenon has been changing as much deeper and hotter wells, frequently with multiple and separated aquifers with different fluid chemistry and temperatures, are being drilled in Iceland, Italy, Kenya, Greece, Japan, USA or Mexico. In such locations, reservoir temperatures often approach and sometimes even exceed the critical point of water (i.e., 374 °C) and much more hostile, corrosion-inducive reservoir fluids are produced. On the example of the Los Humeros geothermal field (LHGF) in the eastern part of the Mexican Volcanic Belt where exploitation of supercritical resources located below the current productive reservoir depths is planned, demand for effective zonal isolation, to prevent potential scaling and corrosion of steel casing strings, is acute. The occurrence of challenges there is related mainly to the significant temperature difference between encountered aquifers, potential interzonal flow and differences in the fluid chemistry (Negrin at el., 1990).

Cement is a porous material that exhibits high compressive and low tensile strength. Many laboratory studies confirm that the tensile strength of various cement types is usually ten times lower than its compressive strength (De Andrade et al., 2016; Nelson & Guillot, 2006). Cement has low permeability, even though porosity may be relatively high due to the very fine pore structure (Odelson et al., 2007). The combined effect of low permeability and tensile strength can lead to serious

mechanical damage of saturated annular cement at temperatures equal or higher than the boiling point of water at depth. Increased porosity of annular cement sheath, often created due to the poorly executed cementing job, results in deterioration of its mechanical and elastic properties, which play an important role especially after the execution of the primary cementing job. The mechanical cement sheath design for long-term performance is a relatively new practice in the petroleum industry (Nelson & Guillot, 2006) and has not yet gone mainstream in the geothermal industry. There, interest in mechanical and elastic parameters of hardened cement other than compressive strength is still low and concepts for cement design, considering the role of debonding, cracks and plastic behavior, etc., are still to be developed. Common wellbore cement design practice assumes that geothermal cement should exhibit a minimum compressive strength of 6.9 MPa and a minimum permeability of 0.1 mD (API Task Group 1985). Studies carried out throughout recent years (Philippacopoulos et al., 2002; Teodoriu et al., 2010; Liu et al., 2017), concluded that even at high compressive strengths, cement might not provide proper zonal isolation. The geothermal industry experiences significant inadequacy of conventional casing and cementing design procedures for high-temperature wells, as testified by failures of the first and the second venture of Iceland Deep Drilling Project (IDDP) in northern and south-western Iceland or steam leakages and incidents of wellhead growth in some production wells within the LHGF.

The success of a good primary cementing job starts with the proper placement of the cement column along the total length of the casing string, in the annulus between a steel pipe and a borehole. This crucial but technically challenging operation is often executed under high temperatures and in naturally fractured reservoirs. Properly executed cementing operation provides a sound cement sheath of low permeability, which excludes any potential fluid migration unless a leakage path exists (Nelson & Guillot, 2006). A badly executed cementing job might result in chimneys, channels or, at some extreme cases, loss of cement into the formation (Loizzo 2014). Fluid sections, entrapped between casing strings or casing and impermeable formations without a possible relief pathway, can expand during the fluid production phase, compromising cement integrity and eventually leading to an undesirable event of casing collapse. An example of this is presented in Figure 10, where, a high temperature well, located within one of the major geothermal fields in Iceland, experienced collapse of a production casing due to the expansion of isolated fluid pockets. Even if a high-quality cement coverage, confirmed by cementing reports, hydraulic tests, and cement evaluation log analysis, is achieved, cement sealing ability might be threatened by the rapidly changing temperature and pressure conditions during later stages of well's life cycle (De Andrade et al., 2016) and debonding at casing-to-cement or cement-to-rock interfaces and/or cement cracks might appear. Therefore, studies on how the mechanical, elastic and thermal properties of the casing-cement-rock system, its geometry, acting far-field stresses, applied wellbore pressures, and temperature conditions influence the cement sheath stresses are important not only for the proper selection of the cement slurry but also for the definition of allowable pressures and temperatures during the well lifecycle. The determination of adequate mechanical properties allows to characterize cement sheath stresses under applied downhole conditions and predict whether, how, and at which depth cement might potentially fail. Wrongly selected parameters might lead to the loss of integrity, even at the early stages of a well's lifecycle.

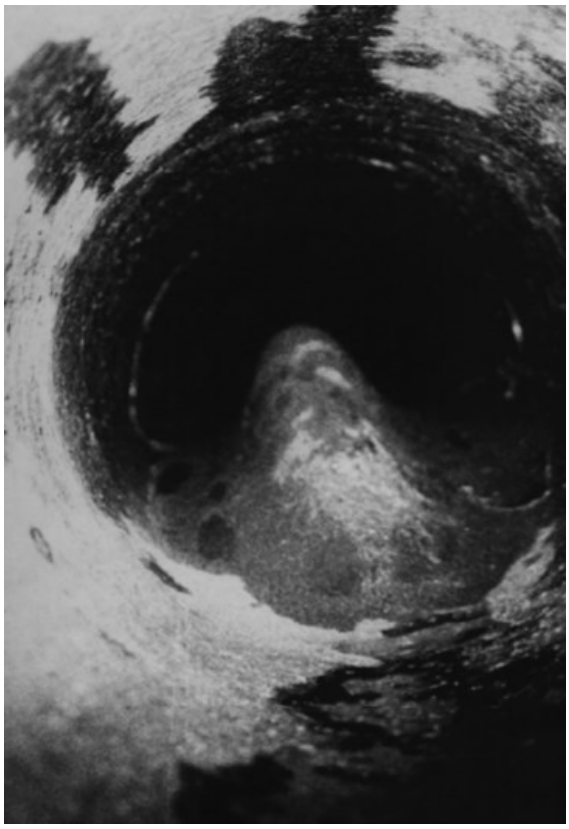

Figure 10: The collapse of a production casing string in a high temperature well in Iceland due to a potential expansion of entrapped water within the annular cement sheath (Thorhallsson 2003).

The first section of the study lists the cement failure modes based on literature studies. The second section describes the theory of cement performance evaluation through the joint interpretation of sonic and ultrasonic wire-line logs, and the influence of microannulus on both recordings; it also presents an interpretation workflow model for the assessment of the mechanical and elastic properties of a hardened cement slurry. The third section introduces the analytical model for cement sheath failure prediction. The next section presents a case study of a 500-meter vertical section of a production casing string from the H-64 well, located in the central part of the LHGF, where maximum wellbore temperature of 395 °C was encountered. The last section describes potential alternatives for conventional Portland cement blends for the future completions of super-hot wells. The study ends with conclusions and well completion recommendations.

3.2. Cement failure

Failure of wellbore cement sheath might be related either to its structure or material. Structural failure includes cement debonding, i.e. so-called microannulus, at either casing-to-cement or cement-to-rock interface caused by high thermo-mechanical post-cementing stresses exerted on the annular cement sheath during operations such as stimulation, injection, fluid production kick-off or well quenching, exceeding material resistance (Wehling 2008). Material mechanical failure manifests itself as chimneys or channels propagating within the bulk of cement (Loizzo 2014). Such failure is usually created once the cement is in a liquid state or during the curing phase, which usually lasts up to 3 to 5 days. The main reason for such defects is faulty execution of drilling operations and/or primary cementing job and includes incomplete cementing due to poor casing centralisation (particularly in

sections of severe doglegs), inadequate drilling fluid removal, contamination with lower density cementing (i.e. spacer) or reservoir fluids (which promotes fluid channelling), cement shrinkage during hydration processes, formation fracturing due to high overpressures, filtration of cement slurry into the adjacent rock formation and inadequate cement slurry selection (Teodoriu et al., 2013). Material failure may also include tensile and shear cracks within the bulk of annular cement created, similar to the debonding scenario, due to high thermo-mechanical stresses created during various operations in the well after the cement is hardened.

Tensile failure

Tensile structural failure of cement sheath, represented by a criterion of maximum tensile strength, assumes that casing-to-cement or cement-to-rock interface will fail, once the tensile radial stresses will overcome the contact strength at cement interfaces or due to significant shear stresses that may evolve. Material failure by the tensile radial cracking will occur once tangential stress will exceed the ultimate tensile strength of hardened cement within its bulk, as the tensile crack propagates perpendicularly to the direction of the maximum tensile stresses (De Andrade et al., 2016; Nelson & Guillot, 2006).

Shear failure

Shear failure of cement sheath occurs once the maximum allowable shear stress is exceeded and it is manifested with local shear cracks within the bulk of cement. To estimate the shear failure of a cement sheath, an assessment of maximum allowable shear stresses is necessary. The most common failure criterion for brittle materials, which are considerably stronger in compression and weaker in tension, is the Mohr-Coulomb criterion (Nelson & Guillot, 2006). It relates the shear failure of the material to its uniaxial compressive strength (UCS) and internal friction angle (De Andrade et al., 2016). Shear stresses can be calculated from the maximum octahedral shear stress criterion (e.g., Von Mises yield criterion). Under the mentioned criterion, compressive shear failure will occur once Von Mises stress exceeds maximum allowable shear stress computed with e.g. Mohr-Coulomb (MC) theory. The cohesive strength and internal friction angle of cured cement are properties that are strongly affected by the cement degradation and are dependent on the water-to-cement ratio and carbonation degree (i.e., cement aging).

Microcracking

Strong degradation of hydrated Portland cement in a form of microcracks occurs at exposure to elevated temperatures especially during geothermal fluid production and the end of the Wait-On-Cement (WOC) period. Such a phenomenon happens due to two main reasons. First, cement has significantly low permeability, even though porosity may be relatively high due to a fine pore structure. Secondly, due to weak tension resistance with even a small increase in the volume of water in the pore space (because of fluid phase change and expansion) creating high enough tensile stresses to cause its mechanical damage. The creation of microcracks leads to increased permeability and a decrease in stiffness and strength. To improve the mechanical properties of annular cement, high-temperature geothermal Portland cement blends rely on various aggregates and additives. The main one is silica flour, which prevents strength retrogression (i.e. the phenomenon of strength decrease, and permeability increase occurring at elevated temperatures). Studies by Odelson et al. (2007) have

shown that around 90 % of hydrated cement stiffness loss occurs below the temperature of 120 °C, regardless of its type. This can be attributed to damage due to microcracking caused by the expansion of pore water in the hardened cement. Microcracking results in permanent deterioration of the elastic properties of hydrated cement at elevated temperatures (Odelson et al., 2007). As it was proven by Xiao & Konig (2004), the Young's modulus of concrete descends linearly with temperature increase. The investigation by Li & Guo (1993) suggested a simple equation for calculation of deterioration of concrete's Young's modulus (E) at exposure temperature between 60 and 700 °C

$$E^T = (0.83 - 0.0011\Delta T) \cdot E \tag{3.1}$$

3.3. Cement performance evaluation

Sonic and ultrasonic acoustic logging tools are commonly used tools for evaluating the quality of annular cement and the degree of bonding at the casing-to-cement interface. Throughout the years, the main procedure was to correlate the attenuation rate of an extensional wave propagating at a sonic frequency (approximately 20 kHz) with the cement compressive strength values using the interpretation chart by Pardue et al. (1963). A later study by Jutten et al. (1989), based on numerous laboratory experiments, proved that it is not the compressive strength but the acoustic impedance that exhibits a high correlation with attenuation rate, regardless of cement type (including lower density cement types). This led to the development of improved interpretation chart correlating attenuation rate, acoustic impedance, and cement's compressive strength. With a fusion and joint interpretation of sonic and ultrasonic measurements, a much clearer picture of cement performance is obtained. It allows for better cement quality evaluation and potential detection of microannulus (Nelson & Guillot, 2006).

Sonic logging

Cement job evaluation is primarily done with the use of cement bond logging tools developed in the late 1950s (Nelson & Guillot, 2006), which throughout the years proved to be sensitive to cement bonding. One of the most popular tools for cement job evaluation is the Cement Bond Log (CBL). Interpretation of such a log is done both qualitatively and quantitively. The first quantitative measurement from the CBL is the transit time of a particular peak of the signal at a receiver, which is measured in microseconds. Such a parameter does not say much about the cement quality as it is used mainly as a quality control only. The second quantitative parameter is the attenuation rate which represents a loss of sound wave energy as the signal travels along with the casing and irradiates energy through the cement sheath. The asymptotic calculation of the attenuation rate, presented in the equation below, was first given by Pardue et al. (1963) and confirmed that the primary cement parameter affecting attenuation rate is wave velocity. It reveals also that attenuation is proportional to the cement density and inversely proportional to the casing thickness.

$$\alpha = \frac{52.2\left(\frac{\rho_c}{\rho_s}\right)\left(\frac{1}{t}\right)}{\left[\left(\frac{V_{pl}}{V_p}\right)^2 - 1\right]^{\frac{1}{2}} + \left[\left(\frac{V_{pl}}{V_s}\right)^2 - 1\right]^{\frac{1}{2}}} \tag{3.2}$$

where ρ_c is the density of cement in g/cc, ρ_s is the density of casing steel in g/cc, t is the casing thickness in inch, V_{pl} is the plate wave velocity in steel in ft/s, V_p is the compressional wave velocity in ft/s, V_s is the shear wave velocity in the cement in ft/s.

Attenuation rate can be calculated from the amplitude at multiple receivers, recorded during sonic logging. Alternatively, it can be approximated comparing the amplitude recorded at a single receiver, located at an axial distance of 3 ft from the transmitter, to the amplitude that would be measured with fluid in the annulus. The CBL mode radiates energy primarily in shear, thus requiring shear coupling between a pipe and an annular solid. The attenuation rate with the liquid-filled annulus (commonly referred to as FPA, i.e. free pipe) is in order of 0.8 db/ft (Pardue et al., 1963), which is around an order of magnitude less than with solid cement.

$$\alpha = -\frac{20}{d} log_{10} \frac{A_1}{(A_1)_{fp}} \tag{3.3}$$

where A_1 is amplitude in mV, $(A_1)_{fp}$ is free pipe amplitude in mV, d is spacing between the transmitter and a single receiver in ft.

Different methods are available for determining values of FPA and 100 % of cement bond amplitude. FPA is a calibration parameter, which is commonly measured during the so-called 'tool check' carried out during wire-line logging operation if a section of unbounded pipe is present in the well. Once no measurement of FPA is available, one can search for sections of pipe with the lowest acoustic impedance (usually the brightest colour on the impedance map) on the ultrasonic cement log correlated with the minimum values at amplitude log. Such sections will imply either FPA or a thick microannulus with fluid filling the free space. Similarly, point with the highest acoustic impedance (usually the darkest colour on an azimuthal impedance map) will serve as a 100 % cement bond value of amplitude. It is worth to notice that FPA depends slightly on temperature and, to some extent, on wellbore pressure. A rule of thumb is that a debonded pipe equals 80 % of FPA (personal communication with Matteo Loizzo). For the H-64 well, investigated in this study, theoretical values from a single receiver of 3 ft (0.914 m) and 9-5/8" casing string amounted to 42 mV for a free pipe and 2 mV for perfect cement bond (Nelson & Guillot, 2006), whereas values recalculated from ultrasonic log amounted to 57 and 14 mV respectively.

As it was proven by Grosmangin et al. (1961), the attenuation rate is directly related, and linearly correlated, to the cement coverage. From this concept, the cement bond index (BI), a third quantitative measurement obtained from the CBL, was derived (Pardue et al., 1963). The BI is a value of the circumferential fraction of cement which is not bound to the casing, manifested as a thin layer of gas or fluid

$$BI = \frac{\alpha_{measured} - \alpha_{fp}}{\alpha_{100\%\ bond} - \alpha_{fp}} \tag{3.4}$$

A BI value of 1 is regarded as a perfect bond between the cement and casing string with a 100 % of cement coverage. For any lower value of BI, there is no full cement coverage, however, the annulus might still be hydraulically sealed. Given the noise affecting measurement at low amplitude and

variation in cement properties, a commonly used criterion for cement sheath isolation is to have 80 % of BI over a given length of pipe (Pardue et al., 1963; Nelson & Guillot, 2006).

Ultrasonic logging

Cement quality analysis is much more refined with the use of azimuthal ultrasonic cement log, which can be explained by sonic log sensitiveness to the microannulus effect. Acoustic impedance acquired from ultrasonic logs is the product of cement density and compressional wave velocity

$$Z = \rho_c V_p \tag{3.5}$$

For primary interpretation of an acoustic impedance log, thresholds for gas-liquid (usually from 0.38 to 1.15 MRayl) and liquid-solid (usually from 2.30 to 2.70 MRayl) interface have to be established. Expected acoustic impedance for low impedance cement is in the range from 2.70 MRayl to 3.85 MRayl, 3.85 MRayl to 5.00 MRayl for medium-impedance cement and above 5.00 MRayl for high-impedance cement (Nelson & Guillot, 2006). A laboratory study by Jutten et al. (1989) on various wellbore cement mixtures using samples cured for one week, found a strong correlation between acoustic impedance and CBL attenuation rate. It was demonstrated, that to do any cross-correlation between different logging and laboratory measurements, the curing time of cement has to exceed 3 days, after which no substantial velocity increase is observed. The application of the correlation by Jutten et al. (1989) is valid for cement slurries with a density varying between 1200 and 2280 kg/m^3. Similarly, to the CBL attenuation rate, an empirical relation between acoustic impedance and cement density was proposed by Jutten et al. (1989). A cement density change might be created during cement mixing due to variations in the ratio between cement powder and mixing water or due to contamination resulting from different low-density fluids (e.g., spacer, tail slurry, displacement fluid) during cement placement.

Using simple equations of linear elasticity with calculated cement density values from an ultrasonic acoustic impedance recording and Poisson's ratio value, the Young's modulus of cement can be obtained

$$E = {V_p}^2 \rho_c \frac{(1+\nu)(1-2\nu)}{(1-\nu)} \tag{3.6}$$

Poisson's ratio values can be easily recalculated using a correlation developed from a laboratory study carried out by Jutten et al. (1989), where a simple empirical relationship between Young's modulus and Poisson's ratio for all tested wellbore cement samples was found

$$\nu = \frac{E+14.9}{3.9E+33.2} \tag{3.7}$$

Influence of microannulus

Microannulus, i.e. deboning at casing-to-cement or cement-to-rock interface, is regarded as a small liquid (wet microannulus) or gas (dry microannulus) filled gap, usually with less than a few hundred micrometers in thickness, created due to pressure and/or temperature changes in the wellbore or faulty cementing job. The presence of microannulus implies that bonding at the interface is lost and in effect, wellbore integrity is threatened. Dry microannuli are created either by formation gas intrusions or by

excessive thermo-mechanical stress resulting from changes in temperature or pressure, whereas water-filled ones are created by the intrusion of reservoir fluids. The dry microannuli are believed to be thinner than water-filled ones (Nelson & Guillot, 2006). In water-bearing systems with high fluid circulation, like most of the productive hydrothermal reservoirs, it is more believed that wet microannuli will be encountered. It is however not necessarily uncommon, to encounter dry microannuli in such conditions, which implies unconnected annular cement defects.

The gas and water-filled microannulus have strong effects on the response of both sonic and ultrasonic recordings and simultaneously make their interpretation much less straightforward (Jutten and Hayman, 1993). The danger of not recognising microannulus in the wellbore might lead to an incorrect assessment of cement soundness and faulty cement behavior evaluation. A different log response is created once dry or wet microannulus is present (Kalyanraman et al., 2017). It is proven that sonic measurements are strongly affected by the presence of wet microannulus, whereas for ultrasonic measurement wet microannulus influence, up to certain gap size, is rather benign. For dry microannulus, sonic as well as ultrasonic measurements might often miss "seeing" cement even with small-scale gaps, however, ultrasonic values drop much faster with dry microannulus size than in the sonic recordings (Jutten & Hayman, 1993; Nelson & Guillot, 2006; Issabekov et al., 2017). Based on a study carried out by Kalyanraman et al. (2017) on the interpretation of sonic and ultrasonic logging results, for properly cemented pipe, values of acoustic impedance from an ultrasonic log (here called ultrasonic acoustic impedance) are similar or slightly higher than values of acoustic impedance recalculated from the sonic log (here called sonic acoustic impedance). For wet microannulus, values of ultrasonic acoustic impedance decrease with decreasing size of microannuli, whereas sonic acoustic impedance stays more or less constant and low. For gas-filled microannulus sonic acoustic impedance values are significantly higher than ultrasonic acoustic impedance values, however only up to approximately 5 μm of debonding (personal communication with Matteo Loizzo).

The low-impedance pixels from the azimuthal impedance cement map are significantly affected by debonding and not by the weaker annular cement behind the steel casing. Therefore, once the presence of microannulus, based on comparative analysis of sonic and ultrasonic logs, is verified one cannot utilize average values of acoustic impedance for recalculating mechanical and elastic properties of annular cement. Such properties are determined primarily by bonding conditions and minimum or average ultrasonic acoustic impedance measurements are therefore not reliable. To carry out computations of cement properties, maximum values of ultrasonic acoustic impedance, less affected by debonding, recalculated from the azimuthal impedance map should be utilized. The procedure of inferring maximum ultrasonic acoustic impedance values assumes counting the pixels on the azimuthal impedance cement map by assigning every pixel impedance value from 0 to maximum acoustic impedance value, usually obtained from Ultrasonic Cement Analyser (UCA). Once such a map is digitalized, minimum, average, and maximum values of ultrasonic acoustic impedance at each given depth point can be assessed. In case when microannulus is not observed, mechanical properties can be inferred from the average values of ultrasonic acoustic impedance.

Interpretation model

To analyse the annular behavior of cement and infer mechanical parameters of annular cement workflow model based on cross-correlations developed by Pardue et al. (1963), Jutten et al. (1989),

Jutten & Hayman (1993), and Kalyanraman et al. (2017) was established. Such a model can provide a much more detailed picture of cement behavior, investigate the presence of microannulus and resolve for the basic mechanical and elastic parameters of hardened cement. It is worth mentioning that, once wet microannulus has been recognised, sonic measurements will not be representative for an annular cement, whereas ultrasonic measurements even with relatively large size wet microannulus are still representative, however, are more easily affected by the presence of even small-scale gas-filled microannulus. The interpretation workflow model is as follows:

1. Establish free pipe and 100 % cement bond amplitude values from an azimuthal ultrasonic bond log in correlation with sonic recordings.
2. Recalculate attenuation from amplitude recordings knowing the sonic (single receiver) tool spacing and free pipe amplitude (Pardue et al., 1963).
3. Calculate the cement Bond Index (BI) using calculated attenuation and free pipe attenuation values with equations given by Pardue et al. (1963).
4. Calculate sonic acoustic impedance with empirical correlation by Jutten et al. (1989) using BI values.
5. Assess regions of liquid-solid, low-medium, and medium-high impedance cement interfaces on sonic and ultrasonic acoustic impedance logs and recognize the presence and type of microannulus.
6. Recalculate cement density, Young's modulus, and Poisson's ratio from correlations given by Jutten et al. (1989) using ultrasonic acoustic impedance.

3.4. Analytical stress model

To calculate potential cement failure, one must calculate the stress state in the wellbore cement sheath. To do so, the analytical axisymmetric model by Ugwu (2008) and Teodoriu (2010), treating the casing-cement-rock as a multi-cylinder setup, was selected (Figure 11). The model, that assumes casing as a thin-walled cylinder and both cement and formation rock as thick wall cylinders, allows accounting for mechanical properties of the casing-cement-rock system, isotropic far-field stresses, applied wellbore pressures and temperature effect (temperature difference between the fluid inside the wellbore and formation temperature). It is widely known, that in-situ stresses most usually are anisotropic, however, the approximation of isotropic far-field stresses, as made in this particular analytical model, is enough to address weaknesses in the annular cement. The casing-cement-rock coupled system is here regarded as a pressurized composite system, without initial stresses existing in cement, with three concentric cylinders and a perfect bonding at casing-to-cement and cement-to-rock interfaces. The casing-cement-rock composite cylinder undergoes plane strain deformation (Ugwu 2008). The assumption was made that the formation rock is impermeable, which is in agreement with the studied LHGF reservoir, where reservoir rocks generally present low porosity and permeability (Aragon-Aguillar et al., 2016).

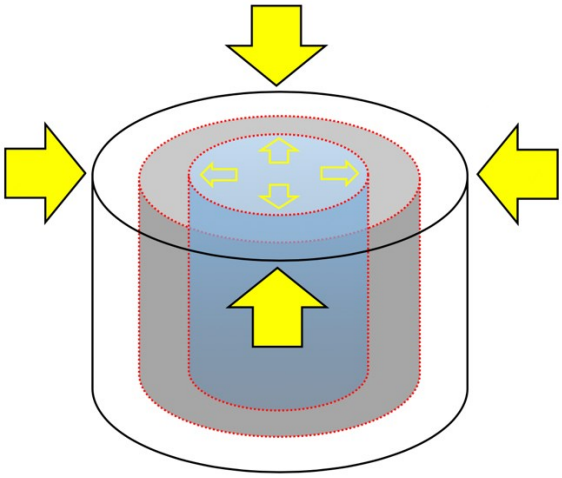

Figure 11: The geometry of the analytical model for the cement failure prediction (red lines signify cement interfaces; yellow arrows signify applied wellbore pressures (empty) and uniform far-field stresses (filled)).

The easiest and most accepted by the industry's way of obtaining far-field stress values is to carry out the in-situ leak-off test (LOT). If results from such tests are not available, as it is the case in this study, horizontal stresses can be approximated by e.g. the Eaton's formula (Eaton et al., 1969) based on values of pore pressure, vertical stress and Poisson's ratio of the formation rocks. For this study, far-field stresses computed in Chapter 2, from this report, were applied. A more detailed investigation of cement sheath stresses and damage propagation would be possible by accounting for anisotropic far-field stresses. A MATLAB software was used for programming of the analytical model and integrating logging data from the case study of the LHGF.

3.5. Case study

Well design

The directional well H-64 was drilled in the central part of the LHGF in the eastern part of Mexico. The kick-off point (KOP) was located at depth of 1000 m with a horizontal displacement of 353 m, final measured depth of 2360 m and true vertical depth of 2310 m. Table 3 presents well design together with casing specifications and setting depths.

Table 3: Casing design of the H-64 well.

Open hole diameter, inch	Casing outer diameter, inch	Casing grade	Casing weight, lb/ft	Casing depth, m
40	30	B	98.93	5
26	20	K-55	54.5	62
17 ½	13 ⅜	K-55	54.5	498
12 ¼	9 ⅝	TN 80–Cr3%	47	1297
8 ½	7 (liner pipe)	TN 80–Cr3%	29	1250 – 1293

8 ½	7 (liner pipe)	TN 80–Cr3%	29	1293 – 2352

Cement slurry properties

Cement used for primary cementation job of 9-5/8" production casing in this case study was class H cement with a density of 1800 kg/m^3 and 40 % BWOC of silica flour, to prevent strength retrogression (Eilers et al., 1983). Additional additives to the cement mixture included defoamers, accelerators, filtration, water loss, and gas control agents and dispersants. The pumpable time for placement of a wet slurry, acquired from the consistometer test results at circulating fluid temperature of 50 °C, amounted to 3 hours and 15 minutes. The cement slurry was designed for the bottom hole temperature of 166 °C. In total 51.45 m^3 of cement slurry was pumped into the well during primary cementing operations (i.e., 31.15 m^3 in the first stage and 20.31 m^3 during the second stage). After primary cement placement, a wire-line logging campaign was carried out including a single 3 ft receiver CBL (sonic) and USIT (ultrasonic) logs up to the depth of 1000 m and six-arm caliper. The sonic and ultrasonic logs were performed on the pressurized well with 3.45 MPa of applied pressure to reduce the thickness of a potentially created microannulus. The logging campaign was carried out 120 hours after the primary cementation job. It can be therefore assumed that all mechanical properties of cement during wire-line logging were fairly stabilized before re-drilling the next well sections. Additionally, the degradation of cement due to hostile reservoir fluids in this particular case of fresh and hardened cement of 5 days can be excluded.

Results from the UCA test, which provide a non-destructive measurement of the relative strength development of a cement sample under defined temperature and pressure conditions, for cement bulk density of 1800 kg/m^3 measured at a temperature of 166 °C give an average impedance of 4.94 MRayls. Such a test serves as a calibration point for the acoustic impedance measurements carried out in-situ. It is worth mentioning, that properties of cement and bonding at interfaces are not constant and change throughout the well life cycle in comparison to rock properties which stay unchanged. Therefore, sonic and ultrasonic logs are only a representation of hardened cement at a particular time. In this case study, it is 120 hours after cement placement.

Model geometry

The model assumes a casing inner diameter of 8.681" and an outer diameter of 9.625" with a wall thickness of 0.472". An inner diameter of cement sheath is equal to the outer diameter of a casing string, whereas the outer diameter of cement sheath, which is simultaneously the inner diameter of rock formations, was assumed as an average value of the minimum and maximum open hole diameter measured by caliper tool. The minimum value of measured caliper amounted to 11.55", whereas maximum value to 13.98", which is approximately 14 % higher than the diameter of the drill bit used in the open hole section of 12.25". The outer diameter of formation rock assumed as 20", is the distance at which the far-field stress condition is linked together to compute the in-situ stress condition, before coupling it with the mechanical properties of the casing-cement system.

Mechanical properties

The Young's modulus of the 9-5/8" production casing material, with a nominal weight of 47 lb/ft and TN 80-Cr3% steel grade was de-rated for the maximum internal wellbore temperature to which steel

was exposed to during various well operations using New Zealand Standard (2015), which can be used for well temperatures up to 350 °C and non-corrosive fluids. Poisson's ratio of casing steel was de-rated for temperature using correlations given by Ancaş (2006), whereas the coefficient of thermal expansion was de-rated for temperature using relation given by Chevron Corporation (2005). It was assumed that the studied 500 m vertical well section was drilled in homogenous formation rock i.e. andesite, with a bulk density of approximately 2540 kg/m^3, an average Young's modulus of 30 GPa and Poisson's ratio of 0.24 (Siratovich et al., 2012). The coefficient of thermal expansion for andesite was obtained from a study by Robertson (1988). The angle of internal friction of cement between 20° (Ochepo et al., 2012) and 57.5° (Fujita et al., 1998) was assumed for the prediction of cement sheath shear failure. The mechanical and thermal parameters of the casing-cement-rock system are given in Table 4.

Table 4: Mechanical and thermal properties of the casing-cement-rock system in the H-64 well.

Component	Material bulk density, kg/m^3	Young's modulus, GPa	Poisson's ratio, -	Coefficient of thermal expansion, 1/K
Casing (i.e., steel at 20 °C)	7700	210	0.30	12E-06
Cement	*see section 3.3*			6E-06
Rock (i.e. andesite)	2540	30	0.24	21E-06

Loading scenarios

Three investigated loading scenarios, imitating the life cycle of the H-64 well are presented in Table 5. The first loading scenario assumes maximum temperatures that cement sheath will be exposed to soon after the calculated curing time (WOC) of five days expires and before re-drilling of the next well section commences. Here temperature and pressure profiles after 7 days of heating-up (i.e. conditions of a closed well) were assumed, as these profiles are the closest to the conditions just after WOC. In this particular case study, it is assumed that hardened cement is not only hydrated but also carbonated enough. For the room temperature, the carbonization of cement takes approximately 28 days, however, in high-temperature conditions and within the CO_2-rich reservoir, such a process will take place much faster. Therefore, cement properties at the end of WOC in the case of the H-64 well should be close to their final values. The second loading scenario assumes the expected production temperature and pressure of a two-phase geothermal fluid at pure water boiling conditions. The exact production temperature is not known, thus assumed temperature amounts to a temperature of a shallow geothermal aquifer in the Los Humeros geothermal reservoir of 260 °C (Verma et al., 1990). The third loading scenario assumes undesirable events of well quenching where internal pressure exerted upon a production casing string is close to the hydrostatic water column with an assumed temperature of killing fluid (i.e., water) is 100 °C.

Table 5: Loading scenarios for cement sheath damage prediction in the H-64 well.

Case		Operation	Temperature	Pressure
I	Drilling	End of WOC time	Heating-up profile 7 days after drilling	Stagnating (heating-up) pressure profile 7 days after drilling operations ceased
II	Production	Fluid production	Temperature of the shallow aquifer of 260 °C	Boiling point water pressure of 4.7 MPa
III	Maintenance	Quenching operation	100 °C	Hydrostatic water column pressure at 100 °C

3.6. Results and discussion

Performance evaluation

Figure 12 presents results from a logging campaign in the H-64 well including mean minimum and maximum borehole width assuming concentric casing and borehole, gamma-ray (GR), travel time, attenuation, ultrasonic acoustic impedance, resolved sonic acoustic impedance, bond index, as well as computed Young's modulus and observed fluid losses during drilling. Cement thickness values are much higher than 0.75 inches (19.05 mm), thus sonic measurements can be regarded as valid (Nelson & Guillot, 2006). Calculated theoretical attenuation for annular cement with Young's modulus of 10 GPa, Poisson ratio of 0.3 and density of 1800 kg/m^3 amounted to 4.95 db/ft, which is significantly higher than attenuation calculated from the amplitude log for the most of the vertical section, excluding short depth intervals at 710 m and between 850 and 875 m, where good cement bond is evident.

Looking at Figure 12, it can be inferred that the well H-64 experiences a wet microannulus i.e. potential cement debonding at the casing-to-cement interface. This can be evidenced by the low values of sonic acoustic impedance recordings, that 'see' liquid in most sections (i.e., values lower than 2.6 MRayl) in relation to the ultrasonic acoustic impedance, which in most parts of the 500 m interval 'sees' low to medium impedance cement with values between 2.6 and 3.85 MRayl and medium to high impedance cement in the last 150 m section. This discrepancy is observed also for BI values calculated from both sonic and ultrasonic logs. A dry microannulus is ruled out due to ultrasonic acoustic impedance values above a typical threshold for gas (~0.5 MRayl) and assumption of high-water circulation in hydrothermal system of which well H-64 is undoubtedly a part. The presence of microannulus is still visible, even with logging operations being carried out on a pressurized well. The de-bonding might have potentially occurred either during or soon after cement curing. The fluid-filled microannulus is most probably caused by a debonding fracture. Therefore, there might be a sizeable liquid layer, which can expand and potentially boil threatening wellbore integrity. The key question for well operators is whether such a layer is isolated or not. Isolated liquid pockets, as mentioned before, will flash and collapse the production casing. However, it is believed that debonding fractures may be connected and pressure might self-regulate either at the source (i.e., deep aquifer), at the surface, or the shallower aquifer.

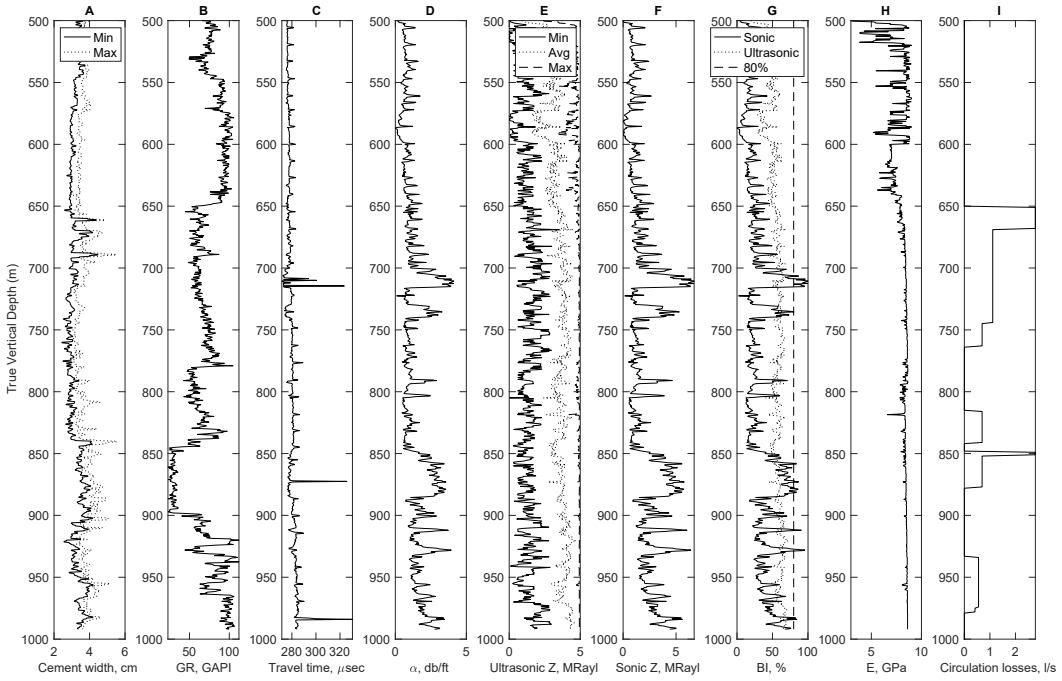

Figure 12: Results of the cement performance evaluation in the 500 m vertical section of the cemented production casing in the H-64 well; A) cement width, B) gamma-ray (GR) log, C) travel time, D) attenuation, E) ultrasonic acoustic impedance, F) sonic acoustic impedance, G) Bond Index (BI), H) Young's modulus, I) observed fluid losses during drilling operations.

Looking at calculated sonic BI values, it can be seen that cement does not achieve good bond and in the majority of the interval amounts to approximately 20 % coverage with slight improvement at latter well sections with BI of around 50 %. However, as it was mentioned before, sonic measurements in the presence of wet microannulus are not representative of an annular cement and thus not reliable. Looking at BI values recalculated from ultrasonic recordings the situation is improved with most of the cemented interval amounting to 50 % of BI with deeper (850 – 1000 m) sections having BI of approximately 60 %. Around the depth of 710 m, an increase in the travel time is seen. This occurrence corresponds to the increase in the sonic attenuation recordings and can be interpreted as the wire-line tool eccentring, as travel time is highly sensitive towards tool centering in the casing string. The section between 850 and 900 m exhibits a strong correlation between the gamma-ray and attenuation values. The gamma-ray log is an indicator of clay fraction (i.e., mostly illite, smectite, chlorite, and kaolinite) in formation rocks (Martínez-Serrano 2002; Nelson & Guillot, 2006). The formation creep is proportional to gamma-ray value and will shrink the casing-to-cement microannulus size leading to higher attenuation and lower apparent cement porosity values, which is seen in this particular well depths. In the mentioned section, a small decrease in ultrasonic acoustic impedance is seen. Additionally, to the cement quality analysis, it is crucial to understand the well history and specifics of the drilling operations carried out in the well H-64. From driller's reports, it is known that during drilling of the 9-5/8" production casing section in the well H-64, partial losses of the drilling fluid occurred (Figure 12). The primary cementing of production casing in, either naturally or drilling-induced, damaged and/or fractured rock formations is much more complex

procedure which may contribute to the incomplete cement coverage around the casing pipe, potentially caused by cement filtration to the adjacent formations, which may have been the case also for the H-64 well.

Failure prediction

Figure 13 to Figure 15 present results of computed stresses within the cement sheath with tensile or shear failure lines, the temperature difference in the vertical 500-meter cemented production casing section in the H-64 well, after the investigation of the loading scenario reported as the case I, II and III representing well life cycle. Compressive stresses are presented in the figures as negative, whereas tensile as positive. Values were smoothed for better data visualisation. In the 1st case, the heating-up temperature and stagnating pressure profiles several days after drilling are considered. Results from this loading scenario, i.e. conditions after WOC time of 120 hours is expired and right before the next well section is being drilled (with wellhead being still closed), indicate that most stresses in the cement sheath remain in compression with an exception of an interval between 600 and 650 m, where both radial and tangential stresses become tensile and exceed the tensile strength of the annular cement. This may lead to a potential tensile failure of the cement sheath in a form of microannulus or radial cracks, related to the high-temperature gradient inside the well and cooler adjacent rock formations. The analysis also proves a shear failure, potentially resulting in debonding at a casing-to-cement interface or local shear cracks, at depths between 600 and 950 m. Contact pressures between cement and rock formations at depths between 750 and 800 m as well as 850 and 1000 m stay below the shear failure line. An interval between 500 and 600 m of depth is not expected to fail due to tensile or shear failure at this particular loading scenario.

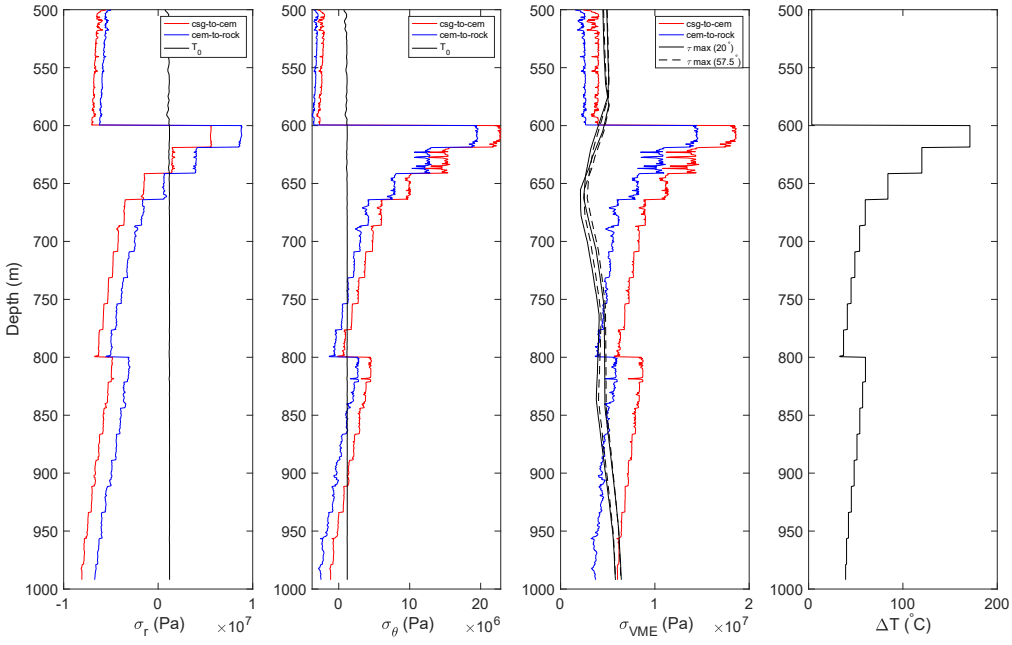

Figure 13: Radial (σ_r), tangential (σ_θ), and VME (σ_{VME}) stresses in the cement sheath of the production section in the H-64 well at the end of WOC.

In the production case scenario, the geothermal fluid production temperature of a shallow reservoir at 260 °C and a water boiling pressure of 4.7 MPa is considered as boundary condition. The tensile failure of the cement sheath is seen for all the principal stresses in the section between 500 and 650 m. A shear failure might extend to a depth of approximately 700 m, leading to potential cement debonding at interfaces or local shear cracks propagating in the tangential direction of the cement-to-casing interface. Below a depth of 750 m, no cement sheath damage is foreseen for a given case scenario of fluid production. In this case, the main factor generating the potential annular cement failure is the temperature difference between the hot geothermal fluid flowing inside the well and the colder surrounding rock formations.

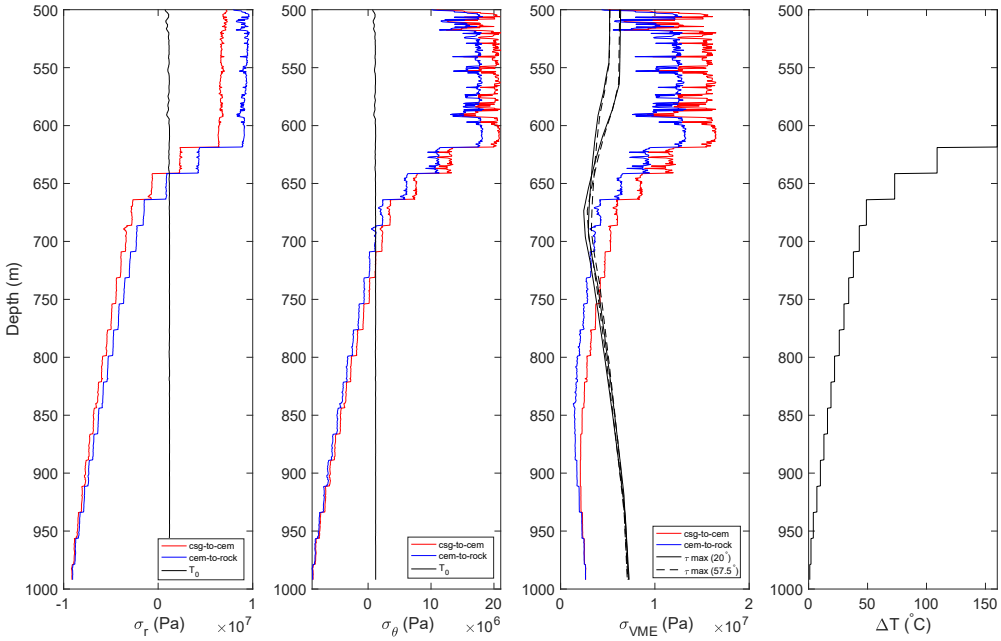

Figure 14: Radial (σ_r), tangential (σ_θ), and VME (σ_{VME}) stresses in the cement sheath of the production section in the H-64 well during geothermal fluid production.

For the maintenance loading scenario, quenching operations down to 100 °C with corresponding hydrostatic water column pressure are taken as the boundary condition. Here, hardened cement prevails undamaged between 500 and 625 m. Below this depth, all stresses become tensile and greatly exceed the tensile strength of annular cement leading to its failure in tensile and shear mode. In this particular loading case, the main factor controlling the potential cement failure is the temperature difference at depth in the quenching phase.

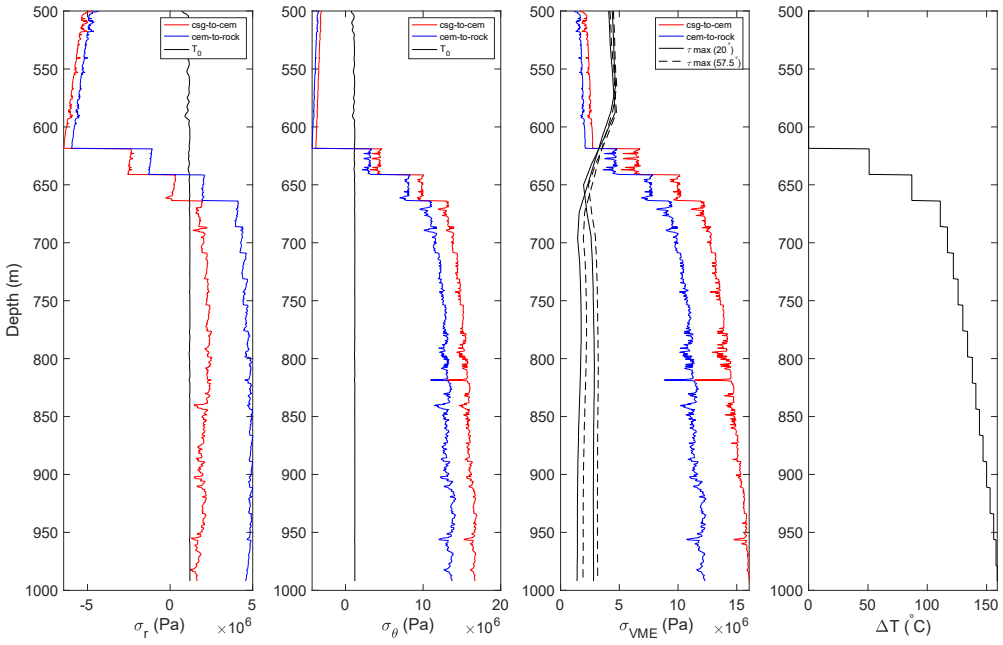

Figure 15: Radial (σ_r), tangential (σ_θ), and VME (σ_{VME}) stresses in the cement sheath of the production section in the H-64 well during well quenching operations.

3.7. Experimental laboratory studies on alternative sealants for completions of super-hot wells

Potential alternative wellbore sealing systems for super-hot wells include non-Portland mixtures. Such systems are still relatively unknown and uncommon for completions of deep high-temperature wells. This is primarily due to the lack of information on the long-term performance of such mixtures in geothermal conditions. In the recent Venelle-2 drilling campaign in the Larderello geothermal field in northern Italy, where supercritical conditions of geothermal brine were being targeted, specially developed non-Portland calcium phosphate sealing system was applied for the primary cementing operations with satisfactory results (Bertani et al., 2018). This proves rising interest in non-Portland blends for high-temperature well applications, especially where corrosive and acidic fluids are expected to be directly in contact with the cement sheath. Such sealing systems might potentially replace conventional Portland blends in the near future once its long-term behaviour in-situ is better understood. Potential alternative non-Portland mixtures, among many others, include alkali-activated aluminosilicates. These so-called geopolymers consist of a base material composed of an aluminium silicate combined with an alkaline solution. Aluminium silicate sources can be natural, such as metakaolin, or industrially produced. Merging of the alkaline solution initiates the formation of a gel-like matrix consisting of different oligometric units, referred to as “polysialates”. Such units form a chain (or a ring) of structured polymers containing Si^{4+} and Al^{3+}. The main structure of the formed oligomers consists of quadratic-planar shaped tetrahedons with a coordination number of 4. The coordination number, often also referred to as ligancy, describes the number of ions, molecules, or atoms that are the closest neighbour in a compound or crystalline structure. The molecular formula of a formed gel always shows the following structure (Duxon et al., 2005)

$$M_p[-(SiO_2)_z - AlO_2]_p \cdot w\ H_2O \quad (3.8)$$

where M is a monovalent alkali metal cation such as Na^+ or K^+, p is the degree of polycondensation, and z is the stage of the sialate (e.g. $z = 2$ describes poly-sialate-siloxo with a structure of -Si-O-Al-O-Si-O) (Rangan & Hardjito, 2005). As seen from the above-mentioned formula, there can be several SiO_2 molecules associated with one AlO_2 molecule. The relation of Si to Al has therefore great influence on the resulting structure. Increasing the Si amount leads to more complex amorphous structures increasing the stability of the gel-phase and determining properties of the resulting material (Davidovits 1991).

In this study, we use industrial aluminium silicate fly ash and silica sand as base materials for creating an alternative sealing system for a potential application in a super-hot geothermal well. Fly ash is a by-product of lignite or black coal combustion, having, therefore, a positive environmental footprint. The hardener mixture of the geopolymer blend, designed especially for this study, consists of an aqueous, eight molar solution of sodium hydroxide (NaOH) and soda water glass ($NaSiO_2$), which is composed of 26.3 % silicate and 7.9 % sodium oxide. To improve the performance and workability of the fresh geopolymer sealants, superplasticizers were added. Comprehensive experimental laboratory studies of non-Portland geopolymer and conventional Ordinary Portland Cement (OPC) (Table 6) sealing systems, representative of a cement blend type used in the LHGF for primary cementing of productive casing strings, were carried out (Glißner & Lefebvre, 2018). Portland cement type used in this study was CEM I 52.5 R NA, where CEM I indicates Portland type cement with up to 5 % of minor additional constituents, 52.5 describes compressive strength achieved after 28 days of cement curing, R indicates rapid cement setting, and NA signifies low alkali cement type. An inorganic phosphate-based type retarder was added to the conventional Portland cement mixture. This type of retarder usually produces higher final cement strengths.

Table 6: Ordinary Portland Cement (OPC) composition based on mixtures used in the LHGF.

Components	*Quantity, kg/m³*	*Bulk density, kg/m³*	*Volume, m³*
CEM I 52.5 R NA	912	3100	0.294
Silica flour (W12)	365	2650	0.138
Cement retarder	9	1210	0.008
Air-filled voids			0.020
Water	540	1000	0.540

Workability

The flow behaviour represents the success of the slurry placement in the wellbore. It was concluded that geopolymers have initially higher flowability than an OPC sample, which later drastically deteriorates. After approximately one hour of the flow test, geopolymer solidifies and becomes not workable. The OPC blend, on the other hand, exhibited rather constant flowability during the test, being workable even after one hour of the measurement.

Strength properties

Curing sealants in atmospheric conditions is not a realistic representation of condition in deep high-temperature boreholes. Under such conditions, Portland cement, as presented in Figure 16, exhibits the highest values of compressive and flexural strength, i.e., 40 MPa and 4.2 MPa respectively, after 7 days of the curing. The geopolymer blend was not cured under atmospheric conditions as it requires higher temperatures to initiate hardening and solidification. For the case of the oven-cured Portland cement samples under temperatures up to 100 °C, where the influence of water evaporation is believed to be negligible, compressive strength satisfies the required strength for the annular cement of 6.9 MPa (API Group 1985). Above the temperature of 120 °C, a clear deterioration in the both compressive and flexural strength of the Portland cement was observed. This is potentially due to quick water evaporation that allows for the cement to acquire higher strength values and which can no longer be contributed to the setting process. Another effect of high temperature is the impact on the cured sealants microstructure. Any closed porosity will be destroyed due to increasing pressure inside the yet unstable structure. Continuous porosity will be formed, decreasing not only the strength but also dramatically increase permeability. One can see a substantial rise of the compressive strength between 1 and 7 days of curing process for the Portland sealants. It is also seen, that a flexural strength approaches values that are too low to allow for a reliable measurement (i.e., close to 0 MPa) at temperatures above 200 °C. This phenomenon means that rapid failure may occur in the hardened cement in the wellbore (i.e., crack propagation or debonding at cement interfaces) under acting thermo-mechanical stresses. For geopolymer samples, as presented in Figure 17, compressive and flexural strength values are visibly more stable and relatively higher than for the case of conventional Portland cement samples.

To obtain the most representative strength values of borehole-like conditions, samples were cured in a reactor under a temperature of 200 °C with vapour pressure of 1.55 MPa. The closed system of the reactor prevents water from evaporation enabling the hardening mixture to acquire higher compressive and flexural strength. A high discrepancy is observed between values of compressive and flexural strength of both sealants, as presented in Figure 16 and Figure 17, between an oven and reactor-cured samples with the latter ones being significantly higher. It can be also seen that, cured in the reactor geopolymer samples show slightly improved compressive and similar flexural strength to the strength acquired by the conventional Portland mixture.

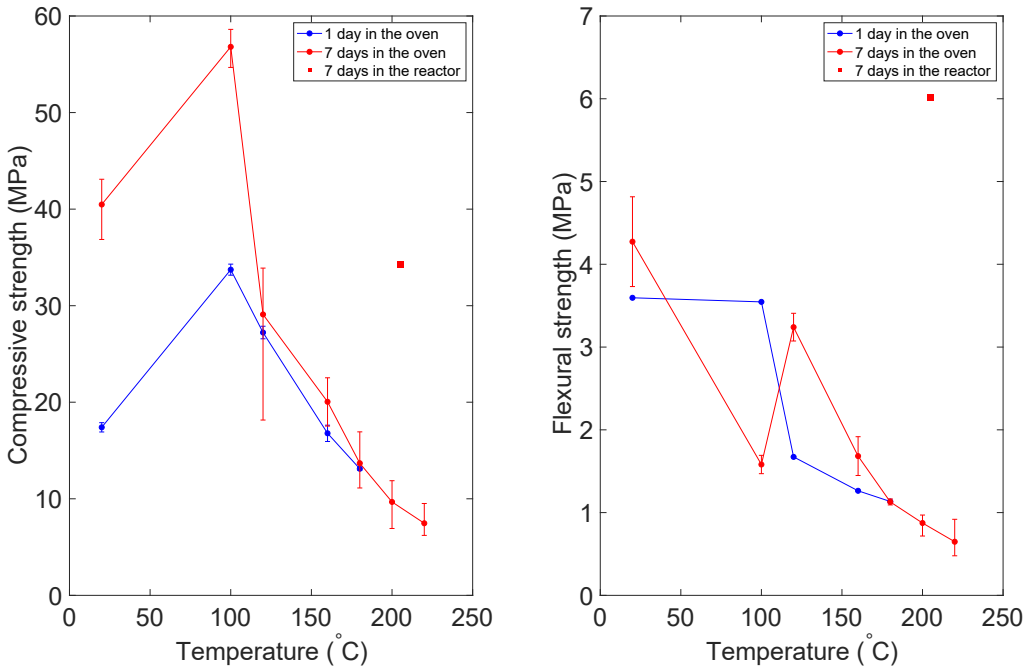

Figure 16: Compressive (left) and flexural (right) strength of OPC samples after 1 day (blue) and 7 days (red) of the curing process at thermal and hydrothermal conditions.

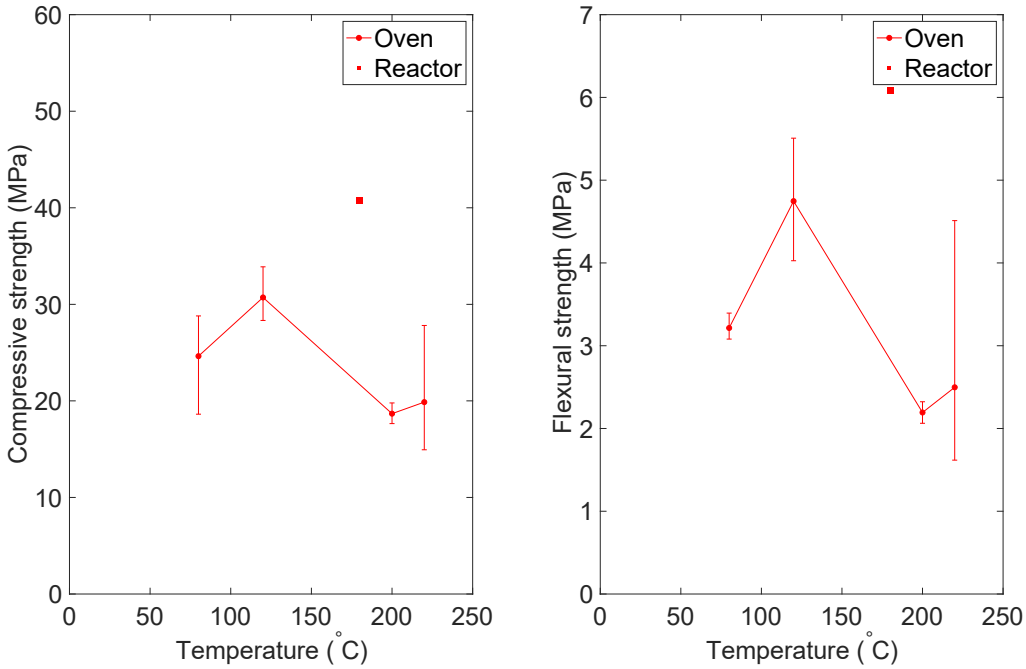

Figure 17: Compressive (left) and flexural (right) strength of geopolymer samples after 7 days of the curing process at thermal and hydrothermal conditions.

Elastic properties

Young's modulus is one of the most important property of annular cement design in high-temperature wells, as it indicates its resistance towards thermo-mechanical cyclic loading. Figure 18 presents results of Young's moduli of OPC and geopolymer sealants cured at different conditions with results

of the Young's moduli of geopolymer sealants after five thermal load cycles with a temperature change from 400 °C to 20 °C.

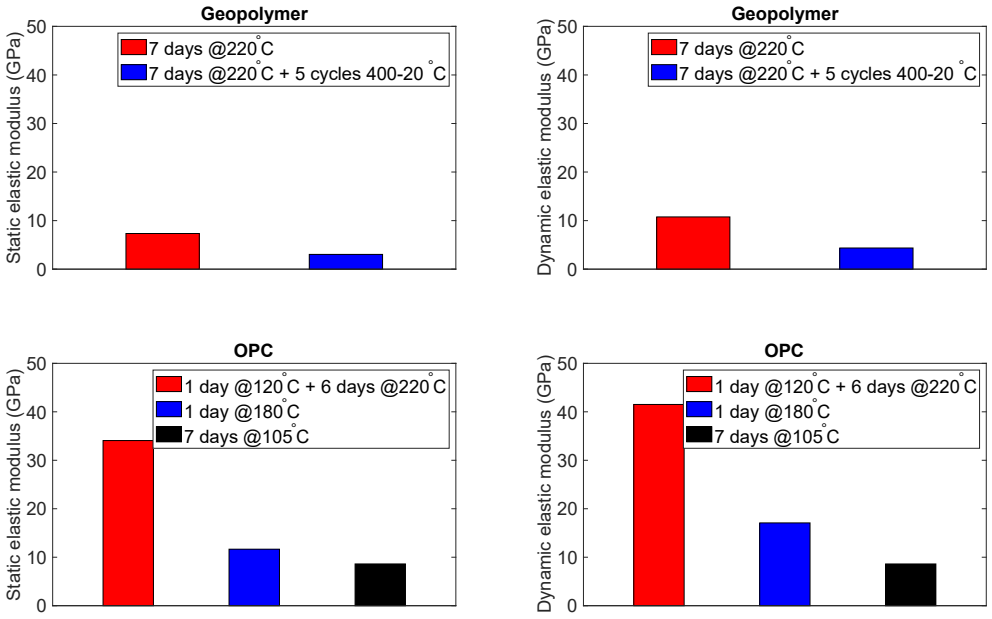

Figure 18: Static (left) and dynamic (right) elastic moduli of the cured OPC (bottom) and geopolymer (top) samples.

The Young's moduli of geopolymer systems is predominantly lower than the one of the OPC systems. This phenomenon would indicate that geopolymers are more ductile and thus more resistant to the potential cyclic loading. It is also seen that after 5 thermal cycles with a temperature change from 400 °C to 20 °C, geopolymer sealants improve their elastic properties, indicated as a decrease of Young's modulus. Young's moduli of the OPC samples are significantly higher than the ones of geopolymers, exhibiting more brittle behaviour and potentially lower resistance to cyclic loading. It is observed that, OPC exhibits much lower elastic modulus after 7 days of curing at a moderate temperature of 105 °C than samples cured just for a day in temperature of 120 °C for 1 day and then 220 °C for next 6 days.

Permeability

It is observed that the geopolymer exhibit slightly improved permeability of 0.0122 mD in comparison with the OPC with permeability of 0.0388 mD. The resulting permeability of both sealants satisfies the required API permeability of 0.1 mD for the annular cement. However, measured values are representative for samples cured for 7 days at 200 °C and 1.55 MPa. It is expected that the values of permeability for longer cured sealants will vary significantly.

Cyclic loading resistance

After a first thermal cycle i.e., rapid temperature changes from 400 °C to 20 °C, the reference OPC mixture showed significant damage, which was visible with a naked eye after sample investigation (Figure 19). After three of such cycles, all of the tested OPC specimens were severely damaged to

the point that the strength test was no longer feasible. Strength measurement of the 7-day cured geopolymer blend after thermal cyclic load tests, i.e. four thermal cycles with temperature change from 400 °C to 20 °C, resulted in compressive strength of 18.9 MPa and flexural strength of 1.8 MPa.

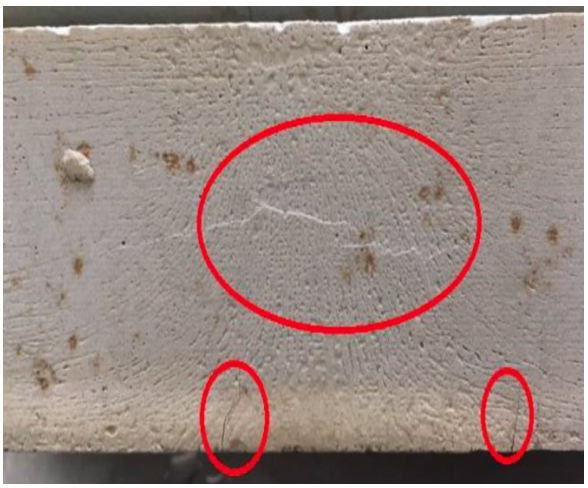

Figure 19:Visible cracks in the OPC samples after one thermal cycle from 400 °C to 20 °C.

Acid resistance

During an acid resistance measurement, a clear reaction of the "acid bath" (i.e., 6 % HCl solution) on the OPC samples, by the formation of a white layer, was visible within a relatively short duration of the test. Mechanical stripping with a spatula led to the detachment of this layer from the cement sample (Figure 20). Below the eroded layer, another dark yellow-brownish one was observed. The geopolymer samples, on the other hand, showed no visual abnormalities and remained untouched by the acid solution. The weight of geopolymers increased by a few percent during an acid resistance test, due to a small amount of an acid fluid filling the pore space in the sample's matrix. The weight of the reference OPC mixture, on the other hand, decreased substantially. Portland cement samples lost about 6 % of their weight after two days during an "acid bath" without any mechanical stripping. Once the eroded outer layer was removed by a light mechanical treatment with a spatula, the weight loss, which might be potentially caused by washing out and erosion resulting from the powerful production fluid flows from deep high-temperature wells, is significantly increased. In the case of geopolymer samples, no removal of the surface was possible even by vigorous mechanical stripping. Thus, the weight loss of geopolymer samples in the "acid bath" is negligible. It was observed that after 21 days of the test, only 61 % of the OPC sample weight and 58 % of its volume is retained.

Figure 20: Results of 7 days of an "acid bath" in a 6% HCl solution (upper row – OPC samples, lower row – geopolymer samples).

Additionally, compressive and flexural strength tests of samples exposed to an "acid bath" were investigated. In the first seven days the compressive strength of the OPC mixture substantially increased. For the case of geopolymer samples, the compressive strength decreases quite sharply within the first 7 days of the test. From the 7th day onwards, geopolymer sealants showed an upward trend, whereas the reference cement mixture a downward trend, of the compressive strength. Despite an increasing compressive strength, a strong downward trend in the flexural strength of geopolymers was observed, similarly to the OPC samples, however with significantly lower strength values. The OPC samples show slightly improved compressive and flexural strength in comparison with the geopolymer samples. This may be potentially due to the water not being able to evaporate from the sample and therefore sufficient amount of fluid is available for the cement curing processes. It is potentially feasible that the low values of flexural strength and relatively moderate values of compressive strength of geopolymer sealant samples might have been connected to the inconsistencies of the acids content while performing the "acid bath" test.

3.8. Conclusions

Cementing of high-temperature geothermal wells is a fundamental procedure that has to be executed properly and supported by detailed stress analysis under expected pressure and temperature conditions throughout different stages of well's life cycle. This study describes an investigation of potential cement damage in a high-temperature geothermal well within the LHGF using an analytical model integrated with azimuthal acoustic measurements of hardened cement. Such analysis gives a very detailed picture of where and how cement sheath might fail and which well sections are the most affected. For a properly designed wellbore cement, in terms of general pressure management, any

possibilities of abrupt temperature changes between well and surrounding rock formations shall be excluded. It was proved that the temperature effect contributes greatly to the stress state in the cement sheath. The drastic temperature changes occurring during the well's life cycle exert high thermal stresses onto cement sheath in the different sections of the well, increasing the probability of failure. The authors suggest to re-consider the well handling procedures in a way that mitigate abrupt temperature jumps in the critical well sections, such as allowing for slow heating and cooling before any well handling. It is believed that, analytical method presented in this paper, together with direct methods of cement sheath quality evaluation such as fibre optic cable, should be used to analyse the long-term wellbore integrity of super-hot geothermal wells in the future drilling campaigns.

To decrease stresses created in the cement sheath during various well operations and prevent premature cement tensile or shear failure, it is advised to improve the elastic properties of the conventional Portland cement blends being used for primary cementing operations or use non-Portland sealants. As it was proven by the experimental laboratory studies, non-Portland geopolymer-based sealing systems exhibit stable and high compressive and flexural strength, good resistance towards thermal cyclic loading, improved ductility with low elastic moduli, acid insensitivity, and improved water permeability, while its self-induced shrinkage remain marginal. Additionally, alkali-activated aluminosilicates sealing systems are economically feasible and their CO_2 emission during the manufacturing process is significantly lower in comparison with conventional Portland sealing systems, making them an environmentally friendly option for completions of future super-hot wells.

References

Ancaş A., Gorbănescu D., Theoretical models in the study of temperature effect on steel mechanical properties, The Bulletin of the Polytechnic Institute of Jassy, 2006.

API Task Group on Cements for Geothermal Wells, API Work Group Reports Field Tests of Geothermal Cements, Oil and Gas Journal, ll, Pages 93-97, February 1985.

Aragón-Aguilar A., Izquierdo-Montalvo G., López-Blanco S., Arellano-Gómez V., Analysis of Heterogeneous Characteristics in A Geothermal Area with Low Permeability and High Temperature, Geoscience Frontiers, Volume 8, Issue 5, Pages 1039-1050, September 2017.

Bertani R., Büsing H., Buske S., Dini A., Hjelstuen M., Luchini M., Manzella A., Nybo R., Rabbel W., Serniotti L., The First Results of the DESCRAMBLE Project, Proceedings of 43rd Workshop of Geothermal Reservoir Engineering Stanford University, Stanford, California, SGP-TR-213 1, February 2018.

Chevron Corporation, Casing/Tubing Design Manual, Chevron Corporation, San Ramon, California, U.S., 2005.

Davidovits J., Geopolymers: inorganic polymeric new material, Journal of Thermal Analysis vol 37, p. 1633-1656, 1991.

De Andrade J., Sangesland S., Cement Sheath Failure Mechanisms: Numerical Estimates to Design for Long-Term Well Integrity, Journal of Petroleum Science and Engineering Volume 147, Pages 682-698, November 2016.

Duxson P., Provis JL., Lukey G.C., Separovic F., van Deventer J.S., 29Si NMR Study of Structural Ordering in Aluminosilicate Geopolymer Gels, Langmuir 21, S. 3028-3036, 2005.

Eaton B.A., Fracture gradient prediction and its application in oilfield operations, Journal of Petroleum Technology, 246, Pages 1353 – 1360, 1969.

Eilers L., Nelson E., Moran L., High-Temperature Cement Compositions-Pectolite, Scawtite, Truscottite, Or Xonotlite: Which Do You Want?, Journal of Petroleum Technology, Pages 1373-1377, July 1983.

Fujita Y., Ishimaru R., Hanai S., Suenaga Y., Study on Internal Friction Angle and Tensile Strength of Plain Concrete, Fracture Mechanics of Concrete Structures Proceedings FRAMCOS-3, 1998.

Glißner M., Lefebvre M., Neue Konzeption von Verfüllungsmaterialien für geothermale Hochtemperaturbohrungen auf Grundlage von Polykondensation, Bachelor Thesis, (unpublished), Hochschule Bochum, International Geothermal Centre (GZB), 2018.

Issabekov Y., Kalyanaraman R.S., Haoua T.B., Benaicha H., Gout O.J., Application of New Interpretation Workflows that Improve Cement Evaluation in Presence of Microannulus, SPE-187461-MS, SPE Annual Technical Conference and Exhibition, 9-11 October, San Antonio, Texas, USA, 2017.

Jutten J.J., Guillot D., Pareevaux P.A., Relationship Between Cement Slurry Composition, Mechanical Properties, and Cement-Bond-Log Output, SPE-16652-PA, SPE Production Engineering, February 1989.

Kalyanraman R.S., Van Kuijk R., Hori H., Making Sense of Why Sometimes Logs Do Not See Cement in the Annulus, SPE Western Regional Meeting, 23-27 April, Bakersfield, California, SPE-185731-MS, 2017.

Kruszewski M., Wittig V., Review of failure modes in supercritical geothermal drilling projects, Geothermal Energy, Science – Society – Technology, 6:28, 2018.

Li W., Guo ZhH., Experimental investigation on strength and deformation of concrete under high temperature (in Chinese), Journal of Building Structures, 14 (1): 8–16, 1993.

Liu W., Yu B., Deng J., Analytical method for evaluating stress field in casing-cement- formation system of oil/gas wells, Applied Mathematics and Mechanics, Volume 38, Issue 9, Pages 1273–1294, September 2017.

Loizzo M., Long-term well integrity: Geothermal energy and annular leak prevention, Conference proceedings from 5th VDI-Fachtagung Geothermische Technologien, Hannover, Germany, 2014.

Martínez-Serrano G.R., Chemical Variations in Hydrothermal Minerals of the Los Humeros Geothermal System, Mexico, Geothermics, Volume 31, Issue 5, Pages 579-612, October 2002.

Negrin L.C.A, Guerra J.C.V., Corrosion and Scaling in the Well H-16 of the Los Humeros Geothermal Field, Vol. 14, Part 11, August 1990.

Nelson B.E., Guillot D., Well Cementing, 2nd Edition, Schlumberger, 2006.

New Zealand Standard: Code of Practise for Deep Geothermal Wells, NZS2403:2015, New Zealand, 2015.

Ochepo J., Stephen O.D., Masbeye O., Effect of Water Cement Ratio on Cohesion and Friction Angle of Expansive Black Clay of Gombe State, Nigeria, Department of Civil Engineering, Vol. 17, 2012.

Odelson J.B., Kerr E.A., Vichit-Vadakan W., Young's modulus of cement paste at elevated temperatures, Cement and Concrete Research, Volume 37, Issue 2, Pages 258-263, February 2007.

Pardue G.H., Morris R.L., Cement Bond Log-A Study of Cement and Casing Variables, SPE-453-PA, Journal of Petroleum Technology, Vol. 15, Issue 5, May 1963.

Philippacopoulos J.A., Berndt L.M., Structural analysis of geothermal well cements, Geothermics, Volume 31, Issue 6, Pages 657-676, December 2002.

Pul S., Ghaffari A., Oztekin E., Hüsem M., Demir S., Experimental Determination of Cohesion and Internal Friction Angle on Conventional Concretes, Materials Journal, Volume 114, Issue 3, Pages 407-416, 2017.

Pulido C.D., Borehole Geophysics and Geology of Well H-43, Los Humeros Geothermal Field, Puebla, México, UNU Geothermal Training Programme, Reports 2008 Number 23, 2008.

Rangan B.V., Hardjito D., Development and Properties of Low-Calcium Fly Ash-Based Geopolymer Concrete, Research Report GC 1, Faculty of Engineering Curtin University of Technology Perth, Australia, 2005.

Robertson E.C., Thermal properties of rocks, U.S. Geological Survey open-file report; Pages 88-441, US Geological Survey, 1988.

Siratovich A.P., Davidson J., Villeneuve M., Gravley D., Kennedy B., Cole J., Wyering L., Price L., Physical and Mechanical Properties of The Rotokawa Andesite from Production Wells Rk 27_L2, Rk 28 And Rk 30, New Zealand Geothermal Workshop 2012, Auckland, New Zealand, 2012.

Teodoriu C., Kosinowski C., Amani M., Schubert J., Shadravan A., Wellbore Integrity and Cement Failure at HPHT Conditions, International Journal of Engineering and Applied Sciences, Vol. 2, No.2, February 2013.

Thorhallsson S., Geothermal Well Operation and Maintenance, Geothermal Training Programme, IGC2003 - Short Course, September 2003.

Ugwu O.I., Cement Fatigue and HPHT Well Integrity with Application to Life of Well Prediction, Master Thesis, Texas A&M University, 2008.

Verma M.P., Verma S.P., Sanvicente H., Temperature Field Simulation with Stratification Model of Magma Chamber Under Los Humeros Caldera, Puebla, Mexico, Geothermics, Volume 19, Issue 2, Pages 187-197, 1990.

Wehling P., Wellbore Cement Integrity Testing, Master Thesis, TU-Clausthal, 2008.

Xiao J., Konig G., Study on concrete at high temperature in China—an overview, Fire Safety Journal 39 (I), Pages 89–103, February 2004.

Coordination Office, GEMex project

Helmholtz-Zentrum Potsdam
Deutsches GeoForschungsZentrum

Telegrafenberg, 14473 Potsdam

Germany